January 2019

Design And Practical Implementation Of Harmonic-Transponder Sensors

Nasser Alkhaldi
Wayne State University, nasser.alkhaldi@wayne.edu

DESIGN AND PRACTICAL IMPLEMENTATION OF COMPACT MICROSTRIP ANTENNAS FOR HARMONIC TRANSPONDERS

by

NASSER S ALKHALDI

DISSERTATION

Submitted to the Graduate School

of Wayne State University,

Detroit, Michigan

in partial fulfillment of the requirements

for the degree of

DOCTOR OF PHILOSOPHY

2019

MAJOR: ELECTRICAL ENGINEERING

Approved By:

_____

Advisor Date

_____

_____

_____

_____

ACKNOWLEDGEMENT

I would like to express my sincere appreciation to Professor Pai-Yen Chen, who contributed great time to my research. Appreciation is also due to Professor Mumtaz Usmen, Professor Lubna Alazzawi, and Professor Nabil Sarhan for their constructive comments and valuable suggestions.

Special thanks to my parents, my brothers and my sister for their love and continuous support. Most of all, I would like to express my appreciation to my wife Latifah for her love and encouragement.

TABLE OF CONTENTS

LIST OF TABLES

LIST OF FIGURES

1 INTRODUCTION

1.1 Motivation

Wireless sensing, tracking and identification platforms have drawn growing interest in the emerging disciplines of internet-of-things (IoTs), autonomous driving, smart health, and smart cities [1,2]. In recent years, passive telemetry based on harmonics detection (e.g., harmonic radar [3,4] and harmonic sensors [5,6]) has been gaining popularity, thanks to its inherent robustness to clutter, jammer, multipath interference, and crosstalk between Tx/Rx antennas. In these nonlinear backscattering systems, a miniature tag or sensor is based on the passive harmonic transponder, which receives a fundamental tone with frequency f_0, doubling its frequency, and re-transmitting the second harmonic with frequency $2f_0$ to interrogators located in a rich scattering environment. Since the reader transmits and receives orthogonal frequencies, the influence of unwanted clutters and multi-patch interferences can be considerably suppressed. Very recently, zero-power, miniaturized harmonic sensors have been proposed for IoTs applications, with low power consumption and long read range [5,6]. A harmonic sensor typically includes a physically/chemically-sensitive sensor that modulates the strength or peak frequency of the backscattered second harmonic [5,6]. Harmonic sensors have been extended to non-invasive detection of critical symbols in medical applications [5,7], and remote sensing of temperature and humidity [6,8].

The overall model of wireless sensing comprises a sensor and a reader scheme. In addition, a practical sensor comprises of a harmonic-transducer, a non-linear component, and an antenna. In some applications, the reader has both receiver (Rx) and the transmitter (Tx) [9]. However, in principle, both components can be separate. Based on the sensing system, the backward and forward communication from sensor to receiver and transmitter to sensor, correspondingly, can happen at similar or unalike frequency bands. A model of a sensor scheme through which two dissimilar frequency bands are utilized for communication is harmonic radar. Regarding the harmonic radar implementation, the tag or sensor

is referred as a harmonic transponder. It collects the interrogation signal at a specific frequency before converting this signal into a harmonic-response-signal at the frequency.

Harmonic radar system was first used in the World War II to identify enemy tanks and aircraft [9]. The use of harmonic radars was first presented during the 1960s [10]. Some of the initial applications were related to automotive uses. Earlier applications of harmonic radar were witnessed in construction when analyzing the corrosion of steel supports specifically in concrete structures. Other earlier applications of harmonic radar include tracking of small amphibians and insects in addition to tracing avalanche victims. Lately, the applications of transponders and harmonic radar are the detection of certain signs in biomedical, remote sensing, and sensing electronic machines, which infringe existing emission restrictions. Although the harmonics-based radar and sensor systems may offer advantages in terms of power and detection range, they usually require two (Rx/Tx) antennas operating at both the fundamental and harmonic frequencies [3, 6]. This unavoidably increases the total device area and cost.

1.2 Limitation of the Related Work

Many applications and projects are using the same as my principle design. Example of these projects are Insect tracking with harmonic radar [11], Chemical or biological applications [12], Strain and crack sensors [13], and Temperature sensor [14]. I deliver more information about these related work in **??** and **??**. In these related work, some of them are using two antennas which one of this antenna sending the signal, and the other one receives it. However, in my proposed design, I use one antenna for sending and receiving the signal. In my design, the two ports with different operation frequencies can be directly connected with the frequency doubler to form the integrated battery-free wireless harmonic transponder. The 3 GHz concentric antenna can receive radiation in free-space, transfer to 6 GHz through the frequency doubler and re-radiate through the 6 GHz inner circular patch antenna. Take a step further, right now we are also preparing to design the frequency dou-

bler on PCB board and shrink the dimension of our antenna again to integrate these parts together to form highly minimized harmonic transponder on single PCB board.

1.3 Objectives

Different from conventional backscatter radar, which receives and retransmit the same frequency signal, harmonic radar can receive fundamental frequency from the transmitter, double the frequency with its integrated frequency doubler and retransmit the second harmonic tone to the receiver antenna. Thanks to this unique feature, harmonic transponder is a effective way to avoid the environment unwanted clutter, noise and even the cross-talk between Tx and Rx antennas.

Even though the harmonics-based radar and sensor systems can provide several advantages in terms of low power consumption and long detection range, they usually require two (Rx/Tx) separate antennas operating at the fundamental and harmonic frequencies, which is not benefit of minimization and integration of the antennas. the main objective of the dissertation is proposed and experimentally validated compact hybrid-fed antenna with the fundamental tone Rx and the second harmonic Tx on one single PCB board, which is benefit of miniaturization of antennas for harmonic radars, harmonic sensors, medical implants, passive radio-frequency identification (RFID), and internet-of-things (IoT) applications.

1.4 Outline of the Dissertation

This dissertation is structured as follows. In Chapter 2, I review the background information about the radar and the harmonic radar transponder sensor. Then, when the harmonic transducer has been used and how it is improved.

In Chapter 3, in order to assist designing the harmonic transducer or sensor, I distribute the important part information of designing a microstrip antenna. It is important to know that Radio frequency identification (RFID) is a type of transponders which respond to interrogations from readers by wirelessly relaying a serial number or a related identifier. The

RFID is type of antenna and because of that, I present the most vital about the antenna basic and the antenna characteristics.

In Chapter 4, I present the methods of analysis for designing the microstrip patch antenna. Micro-strip signifies a form of electrical transmission line that is fabricated by means of printed-circuit-board technology and is applied in transmitting microwave frequency signals.

In Chapter 5, I propose and experimentally validate a compact hybrid-fed microstrip antenna for the harmonics-based radar and sensor systems, which receive the fundamental tone and re-transmit the modulated second harmonic. The proposed microstrip antenna is based on a simple single-layered and dual-feed structure, consisting of an inner circular patch operating in the TM_{110} mode (second harmonic; 6 GHz) and an outer split-ring patch operating in the higher-order TM_{210} or TM_{310} mode (fundamental frequency; 3 GHz).

In Chapter 6, I propose a compact dual-resonant elliptical microstrip patch antenna, employing the even order TM_{c110} mode as fundamental tone receiver and the odd TM_{s110} mode as the second harmonic tone transmitter. Different from conventional harmonic tags using separate antennas at different frequencies, the proposed single-fed elliptical patch antenna can significantly reduce the area occupation and can be designed by an approximate analytical model.

In Chapter 7, I summarize my accomplishments and highlights a conclusion drawn from my work. Also, I provide a future work and how to use my design to implement Harmonic Radar System.

2 BACKGROUND AND LITERATURE REVIEW

2.1 Harmonic Radar

Harmonic Radars represent electrical devices, which illuminate expanses of space with radiofrequency (RF) waves and obtain the harmonics of these transmitted frequencies. The received frequencies are then analyzed to locate the precise positions of the points leading to the production of these harmonics [15]. Radar operation is based on the theory and principles of aspects of radiated electromagnetic (EM) wave. EM waves move across the air at approximately light's speed. The energy of these waves is diffused to and reflected from a targeted entity. A small share of the reflected energy rebounds at the radar set. This rebounded energy is termed as n 'echo' [9]. Radar system analyses the echo to establish mainly the direction and remoteness of the reflecting entity. One of the most significant relationships used in defining the operations of a radar assembly is the radar equation. It identifies the transmitted power in relations to the power received by the radar with respect to antenna dimensions, range, and target scopes.

In a conventional radar system, transmitted electromagnetic pulses are targeted at an orderly environment like the sky [9]. Reflected signals designate the size, position, and remoteness of objects. Conventional radar, nevertheless, is not applicable when detecting objects near or on the ground. The reflected signal of objects on the ground like plants or soil makes target detection difficult. However, harmonic radar technology allows a tag to be attached to the target entity, which enables its position to be established within a disorderly environment. The tag (a small component that can be connected to or combined into a human, item, or insect) comprises of two key elements, which are a wire antenna and a low-barrier-height Schottky barrier diode [9]. The tag relies on the radar signal as a power source and re-radiates a harmonic of the diffused wavelength enabling the emission of a signal in the absence of an onboard energy source. Modifying the receiver to match the harmonic frequency permits the tagged object to be detected from a cluttered background.

In harmonic radar, a transmitter broadcasts a highly polarized beam of electromagnetic waves toward an intended target. Thereafter, the passive entity re-radiates a ray of energy that is harmonically correlated with the polarized transmitted beam back toward the transmitter [15]. Since the receiver is selectively receptive the harmonically linked polarized re-radiated beam, it is protected from blinding that would have resulted from transmitted signals of other redundant targets.

2.2 Harmonic Tansponder Sensor

In the harmonic radar scheme, the tag or the sensor used is referred as a harmonic transponder. It captures interrogation signals at specific fundamental frequency termed as f_0 before converting the signals to harmonic response signals at frequency termed as $_0$ [9]. The symbol n characterizes an integer, which is basic frequency multiplier. Some harmonic transponder implementations found commercially and in works of literature are designed with the help of the second harmonic frequency (2_0) owing to the fact that the finest transponder conversion efficiencies are typically reached at this frequency [9]. On a theoretical level, harmonic transponders are illustrated as comprising antennas and frequency doublers.

As indicated above, a harmonic transponder is made up of an antenna besides a nonlinear element. The nonlinear element can be a Schottky diode, which is responsible for frequency multiplication based on the fundamental frequency of the anticipated harmonic frequency (normally ranging from ($_0$-2_0) [9]. In addition, the nonlinear element ought to convert the power received at the transponder at frequency $_0$ as efficiently as conceivable to frequency 2_0. The antenna is responsible for the communication that transpires between Tx/Rx and transponder. It ought to feed as much as feasible of the power obtainable at $_0$ to the Schottky diode, nonlinear element. It should also be able to emit the power that has been converted to 2_0 as ably as possible back to the receiver. To make this type of operation possible, the antenna must be harmonized both at the second harmonic and at fundamental

frequencies. Other than matching, the backscattering ability of the transponder is influenced by the radar cross section (RCS).

2.3 Literature Review

Radars were the first devices to apply chirp waveform technology. Alimenti and Roselli presented significant works illustrating the concept of theory of the frequency-modulated continuous-wave radar (FMCW) pulses and its radar applications [8]. Following the advancements in electronic circuit systems and signal processing algorithms, radars have found numerous applications like in the field of mobile radio channel classification.

According to Brazee et al., one of the earliest commercial FMCW Harmonic Radar implementation was Metal Target Re-Radiation (METRRA) [16]. The US Army created the system during the late 1970's. The device is designed to identify motionless military targets like vehicles, tanks, and weapon collections that are hidden by vegetation. This system transmits 400 MHz signal and receives it in form of third harmonic (1200 MHz) pulse. It is successful to be used within a range of 1 kilometer. Strategic-Environmental-Research-and-Development Program (SERDP) developed a similar harmonic radar system during the late 1990s. It is used for detection of unexploded ordinance (UXO). It is capable of even detecting and locating buried UXO remotely. Numerous diverse approaches for harmonic generation exist. One popular approach of producing harmonics is through the integration of a non-linear transmission line (NLTL) [14]. NLTL represents a normal micro-strip transmission line, which is occasionally loaded by a variable shunt capacitance. The capacitance is assorted/varied by slotting in a varactor-diode before altering its bias-voltage. This periodic loading transforms the transmission line into a low pass filter that leads to harmonic generation inside the preferred band by restricting the power extended to the higher-level order harmonics [14]. The method also facilitates a wide-ranging impedance bandwidth in addition to aiding impedance matching with antennas.

Another method used in generating harmonics is through a frequency mixer. The mixer

may be executed with the help of a pair of antiparallel Schottky diodes. A configuration achieved through this approach creates only odd term harmonics in addition to the third order harmonic being the main radiated product. The advantages associated with this design are large frequency gap amid the return signal and the interrogation signal as well as the resulting broadband frequency response. The dependence on the third order harmonics, nevertheless, leads to low conversion efficiency.

Harmonic production with better conversion efficiency under no consumption of DC power and with low received RF power can be attained by the use of Schottky diodes. This diode possesses low signal loss properties under high frequencies owing to its low junction capacitance. The key design difficulty is in attaining an adequate match to its large and complex impedances with the use of low-loss and compact matching networks. The diode-reliant harmonic transponder scheme has been utilized in many tracking systems for over three decades. During the year 1980, a transponder design was designed to be utilized in the detection of avalanche victims. This kind of transponder design comprises a pair of rectangular micro-strip patch antennas. Using this design, victims of avalanche buried in snow to a depth of 2.5 m can easily be detected. Rasilainen and Viikari claim that a transponder tag with two half-wave dipole antennas has been designed for tracking bees [17]. Its tag is designed to function at a fundamental frequency of 9.410 GHz. The tag is created using copper plated steel wires. Its frequency multiplication phase comprises a Schottky diode set in parallel with an inductive circuit and has a top conversion efficiency of -33 dB. Lately, harmonic transponders are used in tracking amphibians, specifically in the cryptic stage of their life cycle.

Lazaro Ramon and Girbau claim that for the tracking uses, the harmonic radar system can offer a precise positioning system [6]. Interrogating a movable entity with an attached harmonic transponder permits its direction and distance to be established. Lazaro Ramon and Girbau assert that the location can be achieved through the analysis of power ratio be-

tween receiving and transmitting [6]. Nevertheless, the accurateness and expanse obtained using these methods are very limited owing to system losses and sensitivity of the environmental. The time delay amid the received and the transmitted signals can be evaluated to evade the dependence on the pulse amplitude and boost the accuracy. However, the range is still restricted by the signal width. The frequency modulated continuous wave (FMCW) technique used in radar can also be exploited whenever a high power continuous source is accessible [6]. The accurateness can be improved more using dissimilar coded positioning procedures like the pseudorandom code. Through the application of these codes, it is conceivable to attain a range precision to around 0.1 m in ideal situations.

In modern works of literature, some researchers are attempting to shrink the transponder size besides improving the conversion efficiency using dissimilar antenna design approaches. Mariotti et al. designed a transponder using improved Minkowski loop antennas having fractal geometry [18]. It had tag measures of (0.2 λ $\times$ 0.2 λ)mm and -11 dB as its maximum conversion efficiency. In another experiment, a tag was implemented to have shorted quarter-wave blotch antennas. Its tag measures were (0.21 λ $\times$ 0.1 λ $\times$ 0.006 λ) and -16.7 dB as its top conversion efficiency. Notably, all these designs were limited to altering the transceiver geometry in a planar arrangement and the sensing capability and integration were not resolved.

Other scholars have also explored the rejection of the utilization of a pair of antennas in the harmonic transponder scheme for attaining small footprint. Tsai et al. investigated the use of a dual-band antenna [19]. The research noted that the approach could considerably lessen the generally occupied area. Nevertheless, problems were experienced during the integration of frequency doubler circuit. Rasilainen also investigated the possible use of backscattered harmonics in a study focusing on RFID sensor self-created harmonics [17]. The research noted that the re-radiated harmonics might be utilized in carrying information.

The existing literature on antennas indicates the progressive improvement of antennas

that meet the need for low profiled and compacted communications systems [20]. Currently, antenna designers across the globe are interested in designing compact antennas that have efficient radiation attributes [20]. This literature review indicates that antenna technology emerged during the late 20th century and it has evolved into the contemporary complex field of antennas.

According to Landt, the history of antennas began with the invention of a transmitter by Heinrich Hertz that served as a device to detect electromagnetic waves within the long-wave frequency band [21].

In the 1880, Heinrich performed an experiment to investigate James Clerk Maxwell's assertion that visible light was an electromagnetic wave passing through empty space and air. Hertz constructed a transmitter that comprised two metallic plates and an induction coil connected to two spheres. The experiment was successful because it revealed sparks leaping across gaps of looped wires, indicating the reception of waves. Later in 1896, Guglielmo Marconi constructed the first of wireless telegraphy that involved several antennas for both transmitting and receiving signals [21].

Li claims that antennas that are more complex emerged during the 1920s and it combined several elements in their systematic arrays compared to their predecessors [22]. Metal horn antenna was invented during the 1930s after the inventions of waveguide technologies that could guide the propagation of waves using high-frequency radio signals. Over the years, several improvements of antennas have been developed to suit special purposes.

Kizimenko suggests that in the 1970s, applications of micro-strip antennas, including hybrid-fed antenna and the elliptical patch antenna, in the commercial sector become very popular [23]. The theory of micro-strip antenna first emerged during the 1950s. However, it was not until the 1970s that the first prototype of the micro-strip antenna was fabricated using the printed circuit board. Ever since then, it has become the most preferred type of

antenna in modern communication systems. It has received an extensive range of applications due to its low profile, inexpensive production, planar configurations, and ease of conformal. It has been widely adopted in both military and civilian applications, including broadcast radio, television, radio, satellite communications, surveillance systems, medical field, military systems, radar systems, and radio-frequency identification (RFID).

The hybrid-fed antenna comprises a radiating aperture integrated with a phased array. Hybrid-fed antennas with restricted sector coverage are applicable in fire control systems, weapon detectors, and traffic control systems. Additionally, the applications of the elliptical antenna are becoming more popular in the field of radio engineering.

Bhattacharyya and Shafai (1988) were the first to analyze the annular elliptical ring patch antenna [24]. They used a generalized transmission line model to examine an annular elliptical patch antenna. Their findings indicated that circularly polarized waves could be generated over an extensive frequency range [24]. The study established matching properties between experimental and theoretical characteristics of the elliptical antenna.

3 MICRO-STRIP ANTENNA

3.1 Radio Frequency Identification (RIFDs)

Radio frequency identification (RFID) is a type of transponders, which react to interrogations from readers by wirelessly relaying a serial number or a related identifier. They are commonly applied in tracking items in manufacturing environments and to tag merchandise in stores [8]. It is commonly perceived as an innovative barcode. Nevertheless, its potential area of application is much larger. For instance, it can be used in identifying misplaced items, tracking moving merchandise, and others. RFID tags are anticipated to multiply into the billions in the next few years.

When RFID was first created, it was identified as "Identification Friend or Foe" (IFF) [8]. At the time, the British armies used the technology during the World War II. Transponders were positioned in combatant tanks and planes, and reading devices could interrogate them to establish whether to attack. Heirs of this technology are currently applicable in militaries across the globe. Electronic Article Surveillance (EAS) is among the earliest RFID systems used commercially [8]. It was developed during the 1970s to prevent theft in stores. Its operation relied on tags, which could store single bits. That bit was then read when the client left the store. An alarm would sound whenever the bit was not unfixed. By the end of the 1970s, RFID tags had extended its use into the agricultural sector. It extended to be applied in cataloging animals [8].

RFID transponders/tags comprise of an antennas, microchips, in addition to case batteries only in cases of active tags [10]. The antenna influences the microchip's size. Its form and size are reliant on the frequency of the tag. In addition, the area of use defines the tag's size. It can vary from smaller than a millimeter in implants to book size in container logistic. Other than the microchip, certain transponders/tags contain re-writable built in memory enabling the device to store updates like serialized figures or reading cycles.

In principle, RFID tags or transponders work as indicated below. The reading assembly

creates an electromagnetic field that generates a current in the tag's antenna, which then powers the microchip [10]. Similarly, passive tags use the current to power a condenser facilitating a continuous power supply to the microchip. On the other hand, active tags have batteries that substitute the condensers. After activation, the tag accepts instructions from the reading assembly and response by transmitting the requested information or the serial number [10]. Generally, the tag lacks sufficient energy to generate electromagnetic field on its own. Instead, it exploits backscattering to moderate (absorb/reflect) the field transmitted from the reading assembly.

In a reading phase, the reader continuously powers the tag [10]. This leads to a field of continuous wave, and since the strength of this field lessens with the square of the space, the readers should utilize large power. The field overrides any reaction a tag could provide. Thus, the tag responses via side-channels that are situated just over and under the frequency of this uninterrupted pulse.

3.2 Antenna Basic

An antenna represents a very vital element of any communication system. It is defined as an implement that modifies radio frequency signals, moving across a conductor, into EM signals in an open space [25]. Antennas exhibit an attribute known as reciprocity that implies that this device maintains unchanged properties irrespective if it is receiving or transmitting signals. Some antennas are resonant appliances implying that they function well over a comparatively narrow frequency band. An antenna ought to be tuned to a frequency band matching that of the radio system linked to it, or else the broadcast and the reception will be compromised. Antennas response by emitting radiations that are distributed into space in a specific way when signals are fed into them. A graphical illustration of this relative dispersal of the radiated energy into space is referred as a radiation pattern. The earliest antennas were used in the late 1800's [25]. Heinrich Hertz utilized antennas in some of his demonstrations to show the presence of electromagnetic waves. At the time,

these devices were not operationally or physically isolated from frequency generators. In the 20^{th} century, the antennas were separated from frequency generators, and they were categorized as independent implements in a radio scheme. A RFID reader antenna is designed to transmit a pulse, which has magnetic and electrical properties, electromagnetic waves. In this section, two forms of RFID antennas are illustrated, dipole antennas and patch antennas.

3.2.1 RFID Dipole Antennas

The most projecting use of RFID technology is flow tracking. Since the applications of RFID technology comprise high-reading speed and long-reading range, there is a prerequisite for more exploration into the design of RFID tag antenna [25]. Some applications necessitate that the tags be inexpensive, be compacted in size, and be easy to construct. A RFID dipole antenna is a good contender because it fulfills all these prerequisites. In addition, the far-field emission configuration formed by the dipole antenna is omnidirectional in the entire band of the H-plane permitting constant readability in diverse angles.

A dipole antenna represents the simplest variety of radio frequency antenna. It comprises of a conductive wire pole, which is half the span of the top wavelength an antenna is to produce. The wire pole is divided at the middle. An insulator detaches the two divided sections. Each pole is coupled to a coaxial cable [26]. These types of antennas slope horizontally, vertically, or in inclines. RF current within dipoles is maximum the midpoints of the dipoles. It is at its minimum at split ends of the component.

As indicated above, in RFID dipole antennas the EM waves are transmitted exclusively on one plane, horizontal or vertical, towards the direction of the pulse propagation. This represents ideal wave propagation if the tag placement is identified and fixed. Notably, the antenna and the tag must be harmonized in polarization to get the appropriate read rates.

3.2.2 RFID Patch Antennas

A patch antenna represents a variety of radio frequency antenna having a low profile that can be attached to a leveled surface. It comprises a flat four-sided patch of metal attached to a longer patch of metal [26]. Combined the two patches of metal sheets constitute a resonant portion of a micro-strip transmission line (TL) having a span of roughly one-half wavelength of the radio frequency waves. Its radiation principle rises from breaks at each abridged edge of the micros-trip TL. The radiation from these edges makes the antenna to act largely electrically compared to its physical scopes. Thus, for the device to be resonant, a stretch of micro-strip TL is a little undersized compared to one-half a wavelength of the radio frequency applied.

For a patch antenna, the EM wave is propagated on two planes generating a spherical effect that makes a revolution in a solitary wavelength timeframe [26]. Given the fact that a RFID antenna constantly propagates a wavelength, its rotational field ultimately contacts any tag on its path.

A RFID patch antenna offers a low profile, visually pleasing, inexpensive, and effective design. Patch antennas are also adaptable, conformable, and have reduced sensitivity to production tolerances. These attributes make this type of antennas ideal candidate for applications in RFID. Patch antennas are currently being endorsed for new high-speed RFID Reader Systems [27]. The permittivity of a patch antenna contributes a key role in the general operation of this type of antenna. It influences the width, with respect to the attribute impedance, and the length leading to a reduced transmission efficiency and dissimilar resonant frequency. Patch antennas' radiation efficiency relies on the dielectric's permittivity (ε_r). Preferably, lower ε_r, a thick dielectric, in addition to lower insertion loss is favored for improved efficiency and broadband purposes [27].

3.3 Antenna Characteristics

As mentioned earlier, antennas are responsible for the conversion of one form of a wave into the other. Notably, antennas do not emit/radiate signals correspondingly in all directions. Any antenna radiates radiate more signals in certain directions than others do. The definite pattern relies on the design of the antenna, the environment, and an assortment of other influences. The directional pattern is useful in ensuring that the power emitted is aimed at the anticipated directions [28]. It is usual to denote to the gain or radiated pattern with respect to the transmitted signal. However, an antenna executes its mandate in a precisely corresponding manner for a reception, with matching specifications and figures. To understand the operation of antennas, there are basic characteristics that ought to be defined and clarified.

3.3.1 Radiation Pattern

The radiation pattern of an antenna illustrates the comparative strength of the emitted field in diverse directions by an antenna [28]. An antennas' radiation pattern also refers to its reception pattern because it defines the receiving characteristics of an antenna. Notably, a radiation pattern is represented in three dimensions as shown in figure 1 below. However, the usually assessed radiation outline is a two-dimensional share of its three-dimensional outline, the vertical and horizontal dimensions [28]. The pattern dimensions are exhibited in either a polar or a rectangular arrangement.

Two kinds of radiation patterns are acknowledged (relative patterns and absolute patterns) [29]. Absolute radiation outline is illustrated in using absolute components power or field strength. On the other hand, relative radiation outlines are illustrated using relative elements of power or field strength. Some radiation pattern dimensions are comparative to the isotropous antenna. Through this, the gain transfer approach is used to determine the antenna's absolute gain.

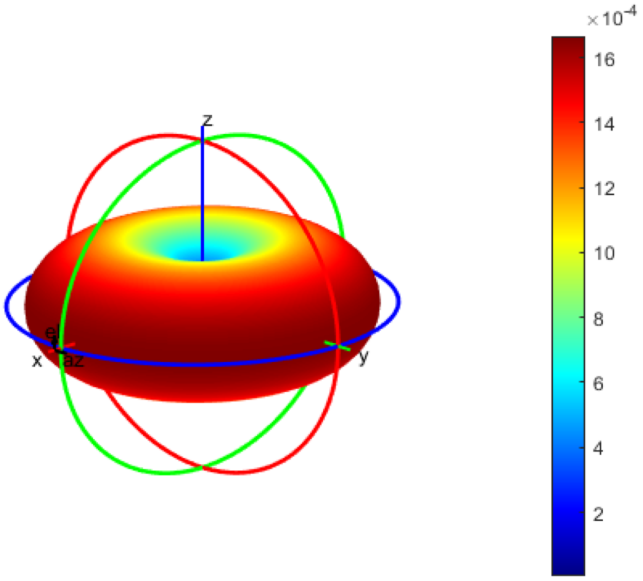

Figure 1: A 3-dimensional radiation pattern of an antenna [30]

At regions far from the antenna, the radiation pattern is different from the areas adjacent to the antenna [29]. A near field represents a radiation field pattern, which is present in areas adjacent to the antenna. On the other hand, far field implies to a radiation field pattern located distant from the antenna. Normally, the technicians are interested in measuring radiated power. This implies that radiation patterns are typically evaluated at the far-field area [31]. When undertaking pattern measurement, it is vital to select a region sufficiently large in the far-field areas. The least allowable distance relies on the antennas' dimensions with respect to the wavelength.

3.3.2 Directivity

Directivity refers to the capability of an antenna to concentrate energy in a specific direction during transmission or to obtain energy efficiently from a specific direction during reception [31]. In a motionless state, it is capable of applying an antenna's directivity to focus the radiated beam in the desired direction. Nevertheless, in a dynamic system that transceiver is movable, the antenna is able to emit energy correspondingly in every direction resulting in an omnidirectional antenna [31]. An antenna's directivity factor, D, refers to a

proportion a radiation intensity, Fmax, resulting from the core direction of emission with respect to radiation intensity, Fi, which would result from a loss-free isotropous radiator under the same emitted power Pt [31]. Its power-density illustrated by a Poynting-vector may substitute its radiation intensity.

3.3.3 Gain

Gain is not an attribute that can be represented in expressions of physical quantities since it represents dimensionless proportions [31]. Gain is presented based on a standard antenna. The most widespread antennas used as reference antennas are resonant-half-wave dipole and isotropous antennas. An isotropic antenna emits energy equally in every direction. Ideal isotropic antennas are not in existent, but they offer important and modest hypothetical antenna patterns for comparing real antennas. A real world antenna emits more energy or waves in specific directions rather than in all directions [31]. Owing to the fact that they cannot generate energy, the entire power emitted is equal as an isotropic antenna implying that in some directions the antenna ought to radiate fewer energy.

An antenna's gain in a specific direction represents the quantity of energy emitted in that direction matched with the quantity of energy an isotropous antenna would emit in the similar direction if powered under the similar input power. Usually, engineers are concerned with the maximum gain that is the gain obtained in the direction, which the device is emitting the most quantity of power. A 3 dB (decibel) antenna gain associated with an isotropous antenna is normally written as 3 dBi (dB gain over an isotropic radiator). A resonant half-wave-dipole may offer a supportive standard for comparison with other antennas under similar frequency or under a much-contracted band of frequencies [31]. A 3 dB antenna gain associated with a dipole antenna is represented as 3 dBd (dB gain over a dipole at the similar height directly above ground).

The technique of measuring gain through comparison of an antenna under examination alongside a recognized standard antenna with a standardized gain is known as a gain trans-

fer method. An additional technique for assessing gain is the three antennas mode. With the help of this approach, the received power and the transmitted power at the antenna terminuses are evaluated between three random antennas stationed at an identified immovable distance.

3.3.4 Return Loss

The return loss presents a means to illustrate a mismatch [31]. It is a representation of a logarithmic ratio gauged in decibels (dB), which likens the power echoed an antenna to the power fed into the input of an antenna from a transmission line. It can be represented as indicated below:

$$Return\ Loss(dB) = \ 10 \ \times \ log_{10}\Big(\frac{P_o}{P_i}\Big) \tag{3.1}$$

$$Return\ Loss(dB) = \ 10 \ \times \ log_{10}\ \Big(\frac{VSWR-1}{VSWR+1}\Big)^2 \tag{3.2}$$

$$Return\ Loss(dB) = \ 20 \ \times \ log_{10}\ \Big(\frac{VSWR-1}{VSWR+1}\Big) \tag{3.3}$$

where the VSWR is stand for Voltage Standing Wave Ratio which is defined as the ratio between maximum and minimum voltage values in the standing wave where:

$$VSWR = \frac{V_{\max}}{V_{\min}}$$

where

$$V_{\max} = V^+ + V^-$$

and

$$V_{\min} = V^+ - V^-$$

Also, return loss can be defined as the difference between the initial forward power and its reflection [32]. The measurement of return loss occurs at the coaxial cable that is connected to the antenna. In mathematical simple format, the power transmitted is assigned PT whereas the reflected power PR. It therefore follows that the return loss is PR/PT which is in ratio format [32]. The ratio dictates the achieving maximum power transfer would require the value of return loss to be as small as possible.

For antennas, the return loss provides the measure of the efficiency of power or signal delivery [33]. Return loss is a positive and dissipative term which acts as a representation of the total reduction of the amplitude of the signal developed from the transmitted power [33]. It is the most convenient way of giving the characterization of mismatches when the reflection is almost negligible. The mathematical amplification increases the value to reasonable values. Also, the use of return loss relate to the Smith chart whose publication dates back to 1939 though updates continued up to 1960s. The chart had nomographs of return loss and reflection coefficient recorded in decibels (dB) [32]. The return loss enables one to determine the accuracy of simulations, measurements, and effectiveness of the reflection of the transmitted signals. Unlike the VSWR bandwidth, the value for return loss establish lower reflection levels [32].

Notably, return loss depends on the configuration of the transmitting surfaces. The shape of the microstrip antenna introduces various limitations that affect the efficiency of reflection of the transmitted power signals [33]. The configuration provides the platform for the feed location which in turn affects the return loss value. Return loss is also affected by length of the U-slot of the microstrip. The other contributing factor is the width ws of the inner U-slot. Comparatively, the variations of these variables directly impact on the value of return loss. The manipulation of the returns loss is possible through the application of the double U-slot in microstrip patch antennas [33]. The design requires simulations using

the CST at the resonance frequency. The optimization of the return loss is necessary to minimize losses and improve signal quality.

3.3.5 Polarization Match

To transmit maximum power amid a transmitting antenna and receiving antenna, both devices ought to possess similar spatial orientation, similar axial ratio, and similar polarization sense [31]. If the antennas fail to line up or fail to have same polarizations, a reduction in power-transfer will be experienced amid the two antennas. The drop in power transfer reduces the general system performance and efficiency [31]. A physical antenna misalignment is expected if both transmission antennas and reception antennas are linearly polarized. Polarization mismatch is calculated using the equation below:

$$Polarization\ Mismatch\ Loss\ (dB) = 20 \times log\ (\cos\ \theta) \tag{3.4}$$

The symbol θ refers to the misalignment slant/angle amid two antennas [31]. The real mismatch loss amid a linear polarized antenna and a circularly polarized antenna will differ based on the circular polarized antenna's axial ratio. When polarizations are corresponding, no attenuation happens owing to coupling mismatch amid the antenna and the field. Whereas, absence in polarization corresponding results in no communication [31].

4 METHODS OF ANALYSIS

4.1 Microwave Micro-strip Circuits

Micro-strip represents a form of electrical transmission line that is fabricated by means of printed-circuit-board technology, and is applied in transmitting microwave frequency signals. It comprises of an electrical conducting stripe detached from a ground plane using a dielectric material called a substrate [34]. Microwave apparatuses just as antennas and filters are usually created using micro-strip, with the whole scheme comprising metallization outline on a substrate. Compared to other waveguide technologies, micro-strip is very cheap, more compact, and lighter. ITT laboratories first designed and created micro-strip in the year 1952 [34]. The drawbacks of micro-strip in relation to other waveguide technologies are the normally reduced power handling capability and higher losses. In addition, unlike waveguides, micro-strips are not enclosed, thus they are disposed to cross talks and unintentional-radiations.

Inexpensively, micro-strip implements can be fabricated on a conventional FR-4 (typical PCB) substrate. It has been established that losses associated with a dielectric in FR4 are very pronounced at microwave frequencies, in addition to dielectric constant not being adequately controlled [34]. Based on these details, a substrate made from alumina is usually used. On a small-scale level, micro-strip TL can also be fabricated into monolithic microwave-integrated circuits. Notably, micro-strip lines are applicable in high-speed digital-PCB designs that require routing of signals from one section of an assembly to the other with least distortion, and avoid high radiation and cross talk. Micro-strip represents one of the numerous types of planar TLs like coplanar waveguide and strip-line [35]. It is possible to incorporate all these types of planar TLs on a similar substrate.

The electromagnetic wave conveyed through a micro-strip line subsists partially in the dielectric substrate as well as partially on the air above the line. Generally, the substrate's dielectric constant will be dissimilar (and higher) compared to that of the air, making the

wave being conveyed to move through an inhomogeneous medium [35]. Consequently, the propagation velocity will vary anywhere amid the speed of radio frequency pulses in air and the speed of radio frequency pulses in the substrate.

Since a portion of micro-strip's fields extends to the air, the real dielectric constant is known as ε_{eff} "Keff" is slightly lower likened with the substrate's dielectric constant. According to Tulintseff and Sorbello, the ε_{eff} of the micro-strip is evaluated using the equation indicated below [36]:

When $\left(\frac{W}{H}\right) < 1$

$$\varepsilon_e = \frac{\varepsilon_r + 1}{2} + \frac{\varepsilon_r - 1}{2}\left[\left(1 + 12\left(\frac{H}{W}\right)\right)^{\frac{-1}{2}} + 0.04\left(1 - \left(\frac{W}{H}\right)\right)^2\right] \tag{4.1}$$

When $\left(\frac{W}{H}\right) \leq 1$

$$\varepsilon_e = \frac{\varepsilon_r + 1}{2} + \frac{\varepsilon_r - 1}{2}\left(1 + 12\left(\frac{H}{W}\right)\right)^{\frac{-1}{2}} \tag{4.2}$$

where;

W: the Width of the feed line.

H: the thickness of the substrate.

4.2 Analytical Model: Resonant Cavity Method

Micro-strip antennas represent planar assemblies, which work as resonant cavities whenever excited. Resonant cavities refer to structures, which permit the accumulation of standing waves. If excited by specific resonant radio frequencies, the cavity leaks from its edges before radiating. Micro-strip antenna, in its modest form, comprises of a thin ($t >> \lambda_0$) metallic patches positioned a slight distance above the ground plane [35]. The ground and patch planar are detached by a dielectric component referred as substrate. Printed circuit methods may be employed to carve the antennas, the patches may take numerous shapes like circular or rectangular, on the substrates to create inexpensive antennas, which have low profiles and incredible resilience to shaking or vibrating environments [35]. In this section, simple rectangular and circular patches are analyzed using based cavity model. The figure 2, below, defines circular patch's geometry. It has a radius " a," a driving point situated at " r," and an angle " θ " evaluated on the x-axis [35].

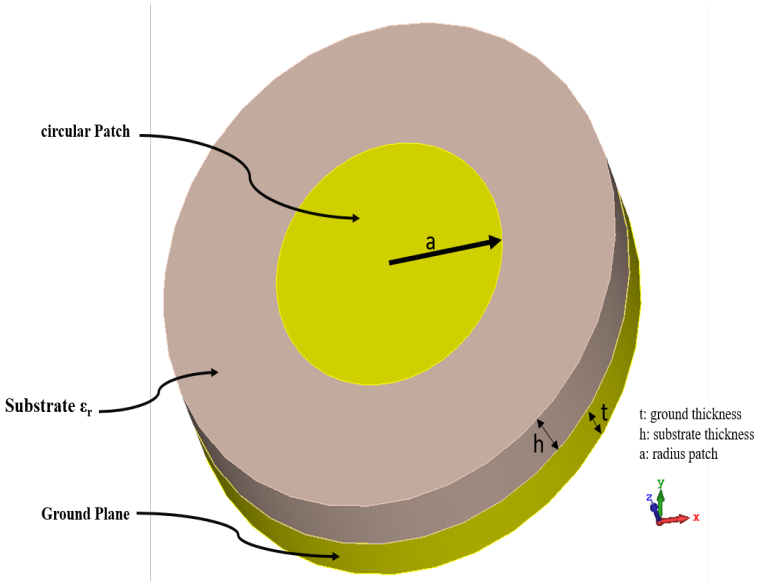

Figure 2: Circular-patch-antenna's geometry

The circular patch is only explored using the cavity model. This can be attained in the same way a rectangular patch is analyzed, but with the help of cylindrical coordinates. Cavity model presents one of the best and simplest techniques to analyze circular patch antenna and may be used to forecast the major few modes' impedance, TM_{11} (transverse magnetic) being the leading mode [37]. The analysis indicates that currently there is a difference between obtained impedances and those published in earliest works of literature owing to the changes in input method used [37, 38]. In the analysis, the impact of loading annular circular antenna can be analyzed. Through this method, the bandwidth of the antenna can be enhanced. Cavity model is applied in the identification of the TM_{np} mode's resonant frequency of a loaded annular circular antenna through shorting posts. In addition, when posts are positioned proportionally the resonant frequency can be investigated [37, 38]. It is indicated that every mode's resonant frequency is reliant on the radial position of the post from the midpoint of the patch antenna and the post's radius. When the post is moved in the direction of the edge of the patch, the TM_{11}'s resonance frequency rises before dropping down [37,39]. The circular patch has input impedance can also be assessed using cavity model. The line below the circular patch creates a capacitive tap with the circular patch on top and ground plane underneath. This input impedance can be investigated using three approaches. The probe-fed circular patch resonator is assessed, then the capacitance is evaluated, and lastly net impedance is distorted at the edge of the line with the help of classical TL transmission.

4.3 New Hybrid-Feed Patch Antenna for Harmonic Sensors

Micro-strip technology's emerging planar outlines are proving to be very vital in the field of antenna and harmonic sensors. Micro-strip antenna facilitates improved repeatability of device parameters like gain, the size of the gadget and bandwidth. A patch outline can be designed any shape ranging from rounded to quadrilateral. The new hybrid-fed patch antenna proposed by Brooker integrates a Pin diode and a Varactor diode [40]. In his

article, Brooker discusses several feeding techniques for the new hybrid-fed patch antenna. The antenna's gain can be enhanced with the help of HFSS software user by Brooker [40]. The figure 3 below illustrates the fields associated with this type on an antenna:

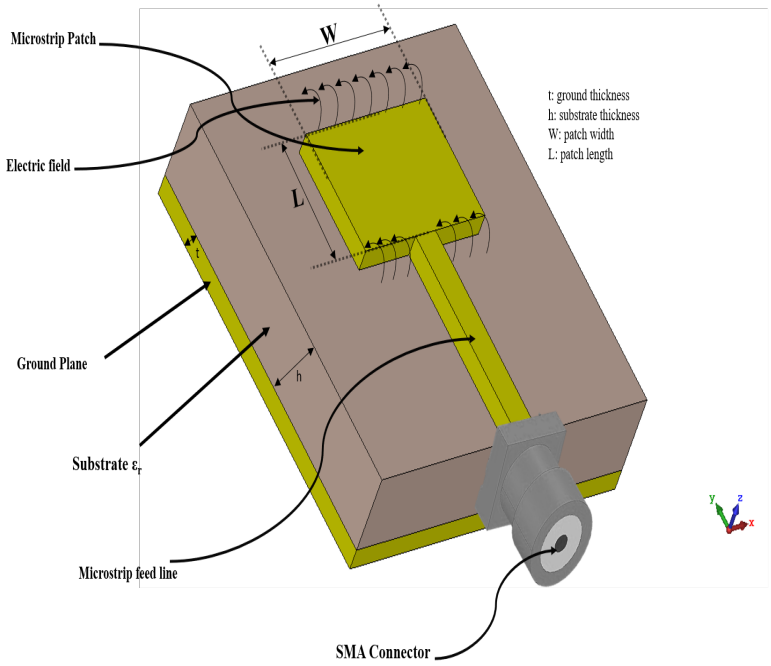

Figure 3: Division of fields associated with new hybrid-feed patch antenna

The dielectric-material is applied in coupling the electromagnetic-energy inside and within the patch. The electric field is at its maximum at one edge of the patch and at a minimum at the other edge of the patch. These maximum and minimum edges are influenced by the input signal [40]. Nevertheless, the electrical field is usually zero at the center of the patch. The electric field inside the patch is drawn-out outside of the patch causing radiation.

4.3.1 Cavity Model

Lao J, Jin R, Geng, and Wu proposed and implemented a novel cavity-modeled probe-fed micro-strip antenna reliant on the theory of hybrid-feed patch [41]. The resultant an-

tenna has a proportioned bandwidth, lower cross-polarization-radiation on its H-plane resulting from its hybrid patch. It is also very cheap since it can be fabricated on an FR4 laminate. Substrate incorporated waveguide technologies are used in the assembly of the metallic cavities.

Conventional micro-strip patch antennas possess distinctive characteristics like lesser volume and conformability with integrated circuits, IC, at a microwave frequency. This has made it a common component in some applications. To attained increased levels of radiation efficiencies, micro-strip antennas are usually designed on a costly low-loss tangent. However, with the availability of this technology for mass-market methods of implementing micro-strip antennas using cheap but electrically compromised FR4 substrates have become common. To address this problem, a novel cavity-modeled probe-fed micro-strip antenna reliant on the theory of hybrid-feed patch has been proposed.

Azenui and Yang proposed an inexpensive cavity-modeled hybrid micro-strip antenna. The device is designed at 2.450 GHz for Inductor Super-Magnetron (ISM) band (2.40 - 2.50 GHz) operation based on zero-input reactance state [42]. This results in a symmetrical bandwidth (based on the operating frequencies) in addition to the real-input impedance (at those frequencies). Currently, the design may be attained with the help of commercial software such as HFSS and MICROWAVE STUDIO. Nevertheless, as their emphasis is on exploration, the design and development procedure become more real if a pre-design (PD) of the geometry being investigated is first found prior optimization using computer simulation technology. Analytical approaches such as the cavity model come in handy for this purpose. However, it would be noted that even though cavity model computes the radiated-field directly using the central resonant-mode TM_{11}, it fails to appropriately account for the asymmetry exhibited by the -plane radiation-pattern of probe-fed reasonably copious hybrid antennas. To account for this, the radiated-fields are evaluated using TM_{10}, TM_{11}, and TM_{12} modes.

4.3.2 Simulation

Theoretical calculations of each antenna are essential before fabrication. The CST microwave studio allows quick and precise analysis of high frequency (HF) components like antennas [43]. It eases the process of designing a structure by providing a 3D modeling auto-flow. After the construction of the model, a fully automatic meshing process is necessary before starting the engine. The CST is mainly used to interconnect all the components of a patch antenna like the substrate, patch, feed-line, and ports before the simulation is commenced. A highly developed visualization engine and supple post-processing enable the scrutiny and advancements of patch antenna designs in suitable and competent ways.

A key benefit of using the CST is its "Complete Technology Approach," which provides the option of mesh or simulator type perfectly matched to a particular problem [44]. No one approach works evenly well in all application spheres, and this regard, the program comprises four distinct simulation techniques (transient solver, frequency domain solver, integral equation solver, and eigen-mode solver) to best complement their exact applications [44]. The most flexible implement is the transient solver because it can reveal the entire broadband frequency performance of the simulated mechanism from a single calculation run, contrasted with the frequency step method of numerous other simulators.

With many independent solver approaches, the CST can solve virtually any antenna application problem. However, despite the solver choice used, some principles of antenna calculations are common [44]. For successful simulation, an antenna project template is selected, units are set, background materials are chosen, the structure is defined, the frequency range is selected. After that "open" boundary conditions are picked, excitation ports are identified, far-field monitors and probes are specified, far-field results processing templates are categorized, prompts appropriate solver are prompted, and results are scrutinized.

After a simulation, the designer can access a range of calculation outcomes are accessed, and the computed output information is retrieved from the problem object tree

situated at the right-hand side of the CST window. To identify a particular port mode, the outputs from the navigation tree are selected [43]. When a specific sub-folder is opened, the magnetic or electric mode field may be chosen. Picking the file for the first mode (e1) will show the port mode and its related limits in the main view [43]. The simulation outcomes will also reveal the central frequency that shows the constant propagation β. Before the fabrication process, the essential results must be highlighted, which are the S-parameter, far-field, polarization quantities, and impedance port resistance that must be around 50 Ω . When the simulation shows all these results as expected, then the patch antennae can be forwarded for the fabrication.

4.3.3 Fabricated Antenna: Eagle PCB Software

After the simulation process, the patch antenna is fabricated using the Eagle PCB, Ki-Cad, or DipTrace. However, this project used the Eagle PCB because it had a better interface compared with the other programs [45]. It represents scriptable "electronic design automation" (EDA) editor with printed circuit board (PCB) outline, schematic capture, auto-router, and computer-assisted manufacturing (CAM) aspects. Using this tool, the project's hardware can be held together by linking and connecting many electronic apparatus jointly on a physical platform.

Other than its resourceful and straightforward interface, educationists, students, and professionals prefer to use EAGLE when fabricating patch antenna because its massive component library cross-platform operates in Windows, Linux, and Mac operating systems [45]. Another advantage of using this program to build micro-strip patch antenna is that it has a modal interface. This feature enables one mode to be picked and operated multiple times, as contrasted to choosing an object and running a single operation at a time. Therefore, when applied appropriately, the fabrication of micro-strip antennas becomes very easy and fast.

The fabrication process begins from the creation of schematic design, which involves

running the Eagle program, selecting new schematic, opening the "add" tools to add various components of the circuit, inserting a potentiometer, grounding the circuit, and connecting the soldering pad. The second step involves the conversion of the schematic into a lay-out, which comprises the opening of a PCB board window to display the components and connections in place. After that, the elements are moved to the designated board area and adjusted to allow traces to be run between them without crossover. The wire button is then clicked to connect the traces. To complete the fabrication process, “gerb274xECESHOP” from the CAM Jobs folder is chosen [45]. Then a new window is opened enabling the fabrication board to be chosen. Five Gerber files will then be created on the same directory with the board file. They are needed for the patch antenna to be fabricated on the PCB and should have extensions of .cmp, .bol, .gbr, .sol, and .gpi.

Once the microstrip patch antenna’s schematic layout and design have been saved on a computer, they can be reused and reproduced many times [46]. Therefore, the use of Eagle program makes it ideal for the creation of several batches of numerous and identical patch antennas. This technical convenience saves time and money ultimately.

5 A COMPACT HYBRID-FED MICROSTRIP ANTENNA FOR THE HARMONICS-BASED

Results from the following studies have been published:

Zhu, Liang, Nasser Alkhaldi, Haysam M. Kadry, Shaolin Liao, and Pai Yen Chen."A Compact Hybrid-Fed Microstrip Antenna for Harmonics-Based Radar and Sensor Systems." *IEEE Antennas and Wireless Propagation Letters* (2018).

In this Chapter, we propose a compact hybrid-fed microstrip patch antenna for the harmonic-based sensing and tracking systems, as schematically shown in figure 4. Different from conventional harmonic tags using separate antennas at different frequencies [47], the proposed hybrid-fed structure can significantly reduce the area occupation and can be designed by an approximate analytical model, with versatile means of modal excitation. In addition, such a design does not require additional filters or diplexers.

we propose and experimentally validate a compact hybrid-fed microstrip antenna for the harmonics-based radar and sensor systems, which receive the fundamental tone and re-transmit the modulated second harmonic. The proposed microstrip antenna is based on a simple single-layered and dual-feed structure, consisting of an inner circular patch operating in the TM_{110} mode (second harmonic; 6 GHz) and an outer split-ring patch operating in the higher-order TM_{210} or TM_{310} mode (fundamental frequency; 3 GHz). By varying the feed position and the geometry of the split-ring patch, specific higher-order mode can be excited at the fundamental frequency. Moreover, analytical expressions were derived for calculating the antenna's resonant frequencies. Our measurement results show that the maximum realized gain is 1.17 dB at 3 GHz and is 3.33 dB at 6 GHz, with good impedance matching (|S11| < -15 dB) and high isolation (< -20 dB).

Although the harmonics-based radar and sensor systems may offer advantages in terms of power and detection range, they usually require two (Rx/Tx) antennas operating at both the fundamental and harmonic frequencies [3, 6]. This unavoidably increases the total

device area and cost.

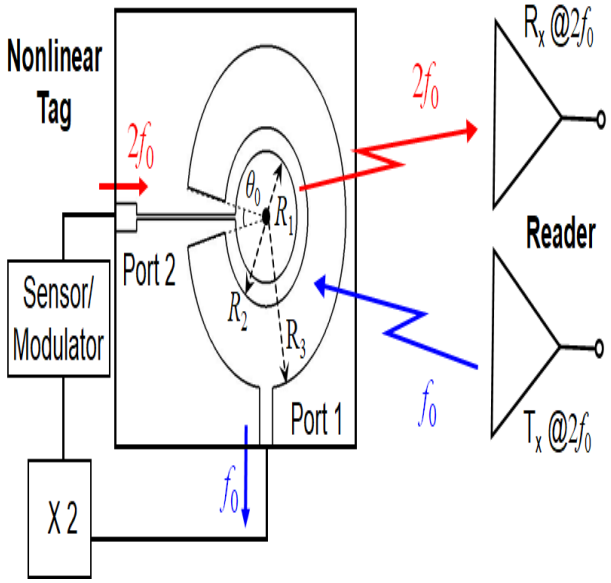

Figure 4: Schematics of a miniature harmonic transponder based on the proposed hybrid-fed microstrip patch antenna

This Chapter is organized as follows. In Section 5.1, we will first use the cavity model to predict resonant modes and modal field distributions of the proposed microstrip patch antenna, which are important for determining positions of the two feed points. Then, we will conduct the full-wave simulation to verify analytical results. In Section 5.2, we will experimentally study the performance of the proposed antennas by fully characterizing their reflection coefficient, isolation, radiation pattern, and antenna gain.

5.1 Design and Simulation

Figure 4 illustrates the geometry of the proposed hybrid-fed microstrip antenna, consisting of a circular patch with radius R_1 and a concentric split-ring patch with inner radius R_2, outer radius R_3, and the cutting angle θ_0. The patch layer is separated from the ground plane by the FR4 substrate with relative permittivity ε_r= 4.3, loss tangent δ = 0.015, and

thickness d = 1.5 mm. The operating frequencies of this hybrid-fed antenna can be estimated by using the cavity model [2], where the circular patch and the split-ring patch resonate at the second harmonic $(2f_0)$ and the fundamental frequency (f_0), respectively.

In each cavity, the perfect electric conductor (PEC) boundary condition is applied at the top and bottom surfaces, and the perfect magnetic conductor (PMC) is assumed on sidewalls. The transcendental equation of the inner cavity, as a function of the radius R_1, can be derived as:

$$J_n^{'}(kR_1) = 0, \; and \; n = 1, \; 2, \; 3K \tag{5.1}$$

where $J_n^{'}(.)$ and $Y_n^{'}(.)$ are the Bessel functions of first and second kinds,k = $\omega\sqrt{\varepsilon_r\varepsilon_0 u_0}$, ε_0 and u_0 are free-space permittivity and permeability. The transcendental equation of the outer cavity, as a function of the radii R_2 and R_3, and the cutting angle θ_0, can be derived as:

$$J_n^{'}(kR_2)Y_n^{'}(kR_3) - J_n^{'}(kR_3)Y_n^{'}(kR_2) = 0, \tag{5.2a}$$

$$n = m\frac{\pi}{2\pi - \theta_0}, \; and \; m = 1, \; 2, \; 3K \tag{5.2b}$$

For the inner circular-patch antenna, the fundamental mode (TM_{110}) is excited at the output frequency $2f_0$, which is controlled by the radius of the circular patch R_1 [Eq.(5.1)]. Depending on the feed position, the higher-order modes (TM_{210} or TM_{310}) can be excited in the concentric split-ring patch antenna, which governs the input frequency f_0 and is tuned by geometrical parameters (R_2, R_3, θ_0) [Eq.(5.2a),(5.2b)].

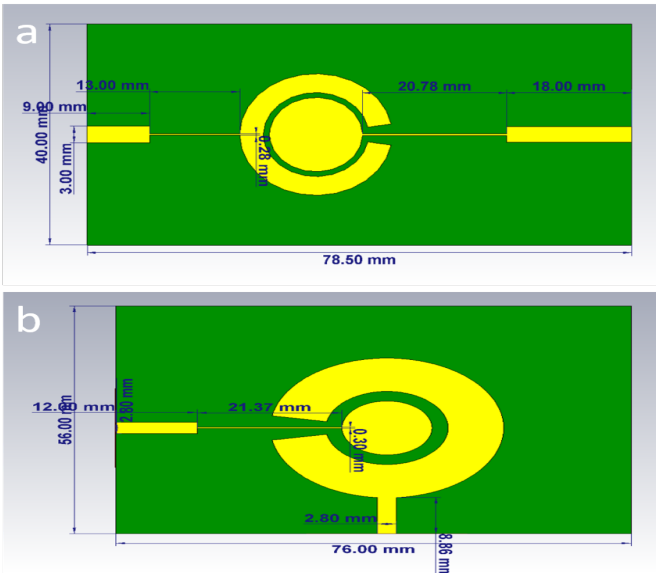

Figure 5: Second and Third mode designed by CST

We have designed the compact dual-fed patch antenna figure 5 for a harmonic transponder is designed to receives a fundamental tone at 3 GHz and retransmits a harmonic signal at 6 GHz. The feed position is of importance, as it determines the excitation of specific TM_{mn0} modes. Here, Eqs. (5.1) and (5.2a) were used to determine the geometrical parameters of the hybrid-fed microstrip antenna. To excite the TM_{210} mode at the fundamental frequency (3 GHz), the parameters of the concentric, split annular-ring patch as it shows in figure 5 (a) are: R_2 = 7.6 mm, R_3 = 11 mm, and $\theta_0 = 20^\circ$. Assuming that the operating frequency is the same, the TM_{310} mode is excited when the geometrical parameters as it shows in figure 5 (b) are: R_2 = 9 mm, R_3 = 17.2 mm, and $\theta_0 = 20^\circ$. To excite the TM_{110} mode at the second harmonic (6 GHz), the radius of the circular patch R_1 = 7 mm. Here, we note that by optimizing dimensions of the split-ring patch (e.g., R_2 = 3 mm and R_3 = 7 mm) is noted that, the fundamental mode (TM_{110} mode) can also be excited at 3 GHz. However, the inner/outer radius of the split-ring patch becomes smaller than the radius of the circular path. In this case, the hybrid-fed structure is not feasible. On the other hand, for higher-order resonant modes (e.g, TM_{410} and beyond), the surface current distributions

and thus radiation pattern become sophisticated, with a reduced broadside directivity and undesired sidelobes.

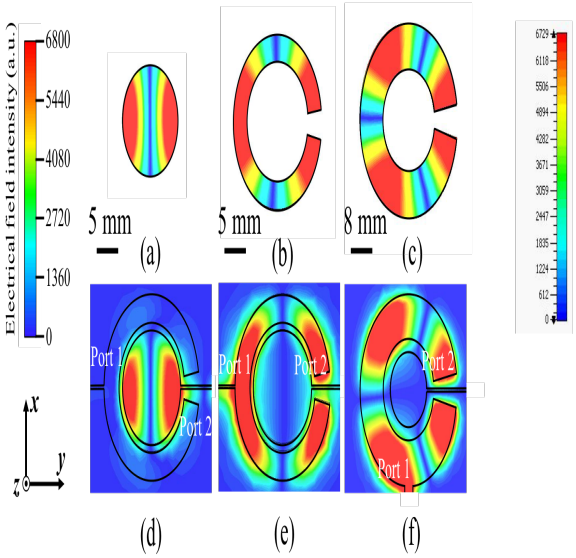

Figure 6: Electric Field (E_z) distributions

We have conducted the full-wave numerical simulation based on the frequency-domain finite-element method to validate the resonant frequencies predicted by the cavity model [48]. Based on the analytical eigenmodal analysis in figure 6 which shows Snapshots of electric field (E_z) distributions for (a) the TM_{110} mode of a circular-shape cavity, and (b) the TM_{210} mode and (c) the TM_{310} mode of the split annular-ring cavity; here PEC boundaries are assumed at the top and bottom surfaces, while PMC boundaries are assumed on the sidewall. we have designed two hybrid-fed patch antennas (TM_{110}-TM_{210} or TM_{110}-TM_{310}) that are fed by microstrip lines connected to two 50 Ω excitation ports (e.g., SMA connector), with suitably designed matching networks. By adjusting the feed point location and the geometry of the split-ring patch, the TM_{210} or TM_{310} mode can be excited at the same frequency (3 GHz). For each mode, the optimum position of the feed point can be obtained by observing the location of maximum field intensities in figure 6(b)-(c). The cal-

culated snapshots of electric field distributions at the resonance frequencies are presented figure 6 (d)-(f), in comparison with analytical results in figure 6 (a)-(c). Here, we find a good agreement between the full-wave simulation results of the realistic hybrid-fed antennas [figure 6 (d)-(f)] and those obtained from the analytical eigenmodal analysis [figure 6 (a)-(c)]. Such results demonstrate the effectiveness of our analytical approach.

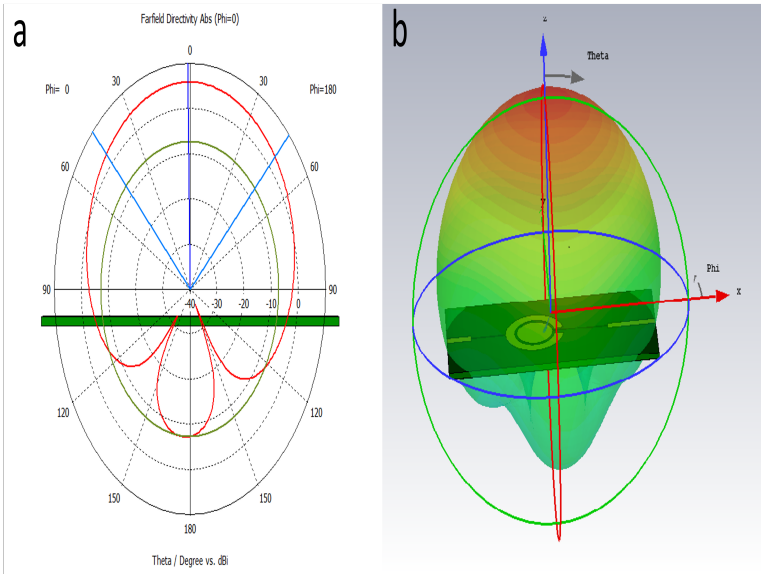

Figure 7: Radiation pattern directivity 3 GHz second modes

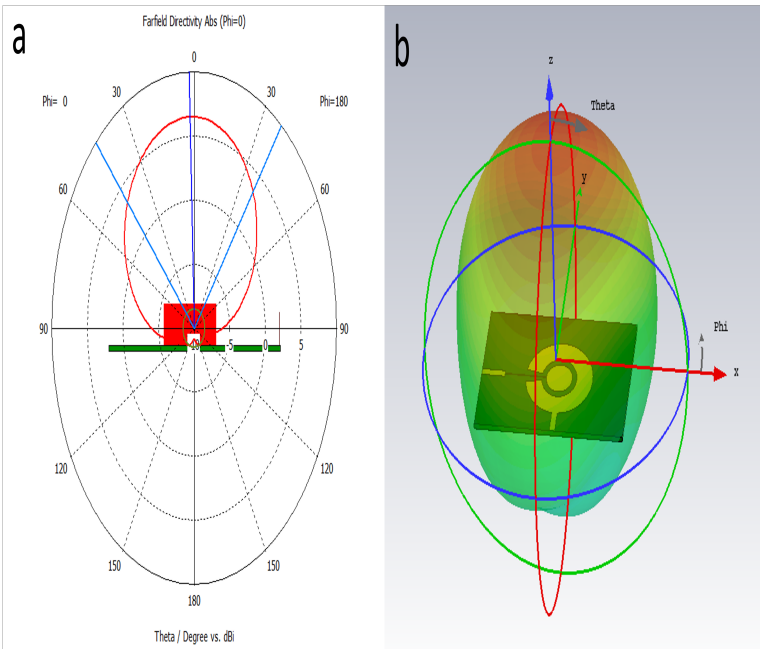

Figure 8: Radiation pattern directivity 3 GHz third modes

In the simulation (CST), after we find the right position for the strip line to feed the patches, the design operated as required. Then, S_{11} represented the fundamental f_0 resonance frequency of the 3 GHz for port 1, and S_{22} represented the second harmonic $2f_0$ resonance frequency of 6 GHz. The radiation pattern directivity for the 3 GHz was perfect and perpendicular to the antenna for the second mode and third mode, as indicated in figure 7 and figure 8. where [figure 7 (a) represented the polar radiation pattern directivity for the second mode - (b) represented the 3D radiation pattern directivity for the second mode]. while, [figure 8 (a) represented the polar radiation pattern directivity for the third mode - (b) represented the 3D radiation pattern directivity for the third mode.]

However, there was a problem with the radiation pattern for the S_{22} for both of its modes because they did not radiate perpendicular to the antenna, as indicated by figure 9 and figure 10. where [figure 9 ghz (a) represented the polar radiation pattern directivity for the second mode - (b) represented the 3D radiation pattern directivity for the second mode]. while, [figure 10 ghz (a) represented the polar radiation pattern directivity for the

third mode - (b) represented the 3D radiation pattern directivity for the third mode].

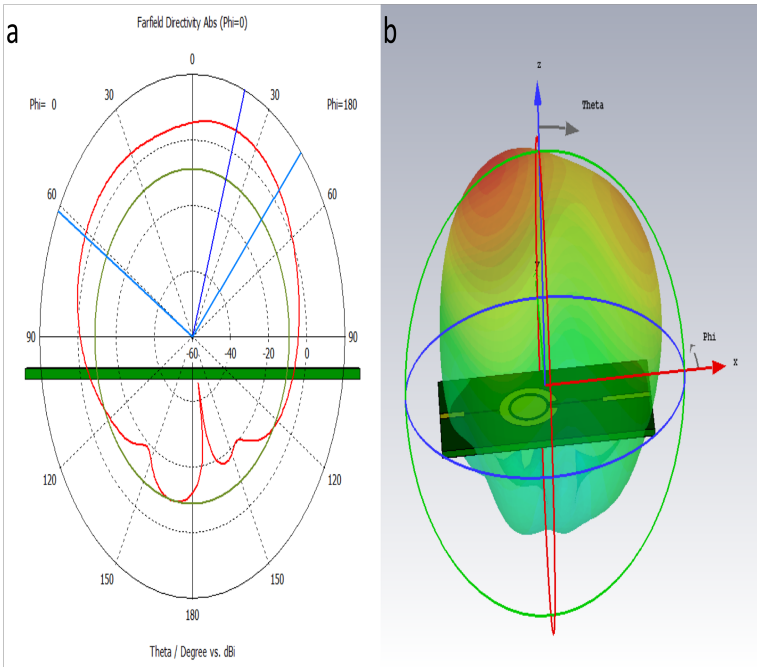

Figure 9: Radiation pattern directivity 6 GHz second modes

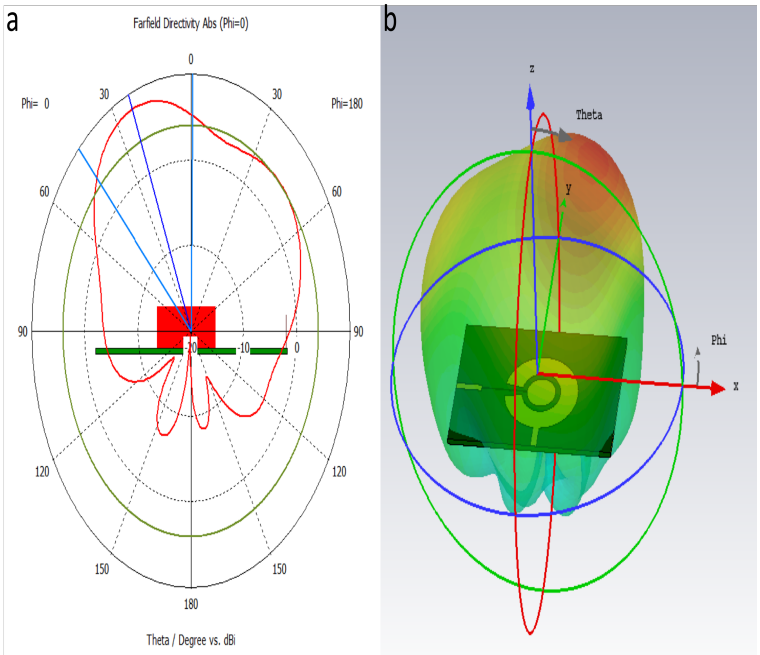

Figure 10: Radiation pattern directivity 6 GHz third modes

Thus, we should solve the problem in order to make the antennas operate effectively with no errors. Existing literature indicated that we could solve the problem by cutting slots on the patch antenna. Therefore, in this experiment, we cut a slot on the inner circular patch operating in the TM_{110} mode (second harmonic; 6 GHz) for both modes. Additionally, we made a small slot on the split ring to enhance its efficiency. After the completion of the new simulation design, the result illustrations on the CST displayed a perfect directivity for both modes, as indicated by figure 11.

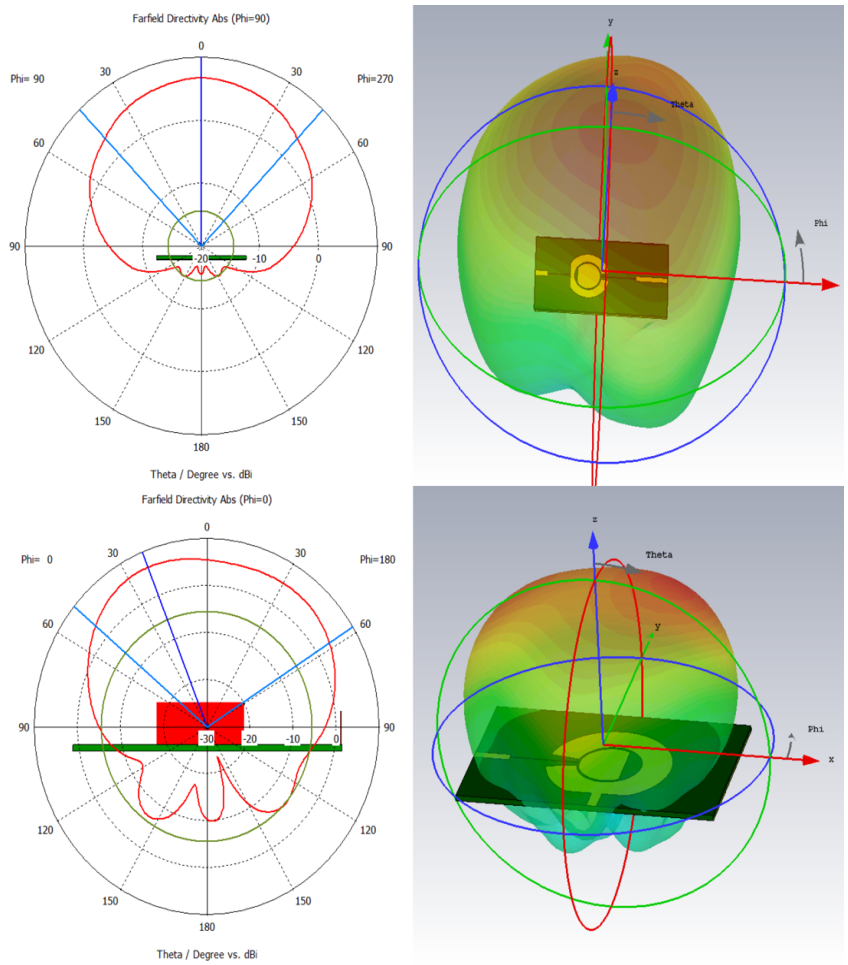

Figure 11: Radiation pattern directivity 6 GHz both modes with cutting slot

5.2 Measurement Results

Based on the theoretical and numerical results indicated in section 5.1, we have fabricated and characterized four different types of hybrid-fed antenna for miniature harmonic transponders. Figure 12 indicates the antenna after fabrication and a test applied on it. To test an antenna, a couple of components are necessary, including microwave amplifier, network analyzer, s-parameter, synthesized sweeper, spectrum analyzer, reader antenna (horn antenna) and the fabricated antenna.

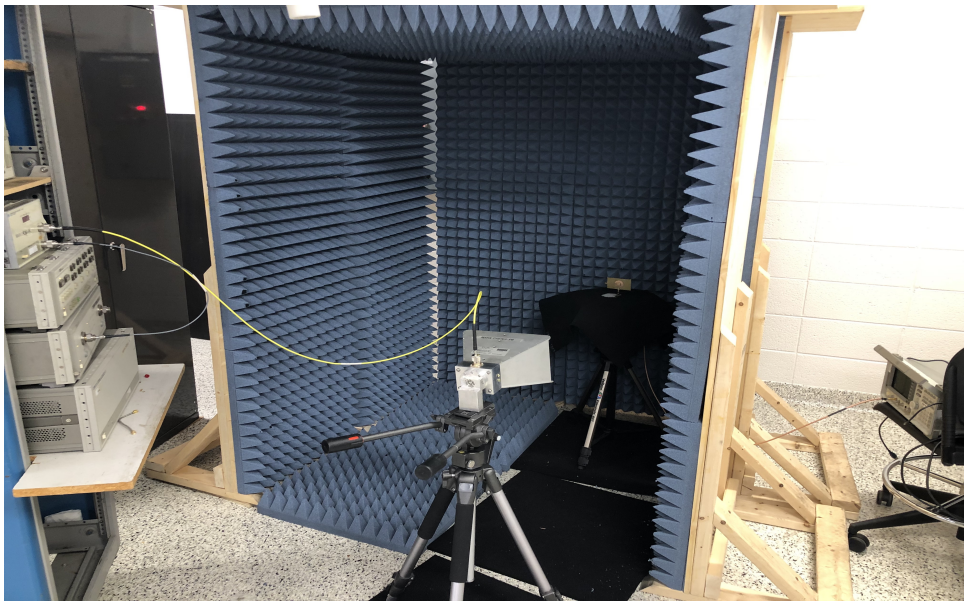

Figure 12: Fabricated antenna under the test

During the test, the components were connected using the following steps:

- The synthesized sweeper, S-parameter test, and the network analyzer were connected.
- Thereafter, the amplifier was connected to the horn antenna.
- Afterwards, the fabricated antenna was placed in front of the horn antenna to enable it to receive a signals.

- Lastly, the fabricated antenna was connected to the spectrum analyzer through the port which needed the test.

5.2.1 Hybrid-Fed TM_{110}-TM_{210} Microstrip Patch Antennas

We have fabricated the proposed microstrip antenna using the low-cost printed-circuit board (PCB) technique, with FR4 substrate and copper (Cu) microstrips. Figure 13 shows the fabricated hybrid-fed TM_{110}-TM_{210} patch antenna in figure 6 (e); here, the received fundamental tone will be guided to port 1 and the frequency-doubled RF signal will be re-radiated through port 2. Figure 14 reports simulated (solid lines) and measured (dashed lines) reflection coefficients, S_{11} versus frequency for the microstrip antenna in Figure 13.

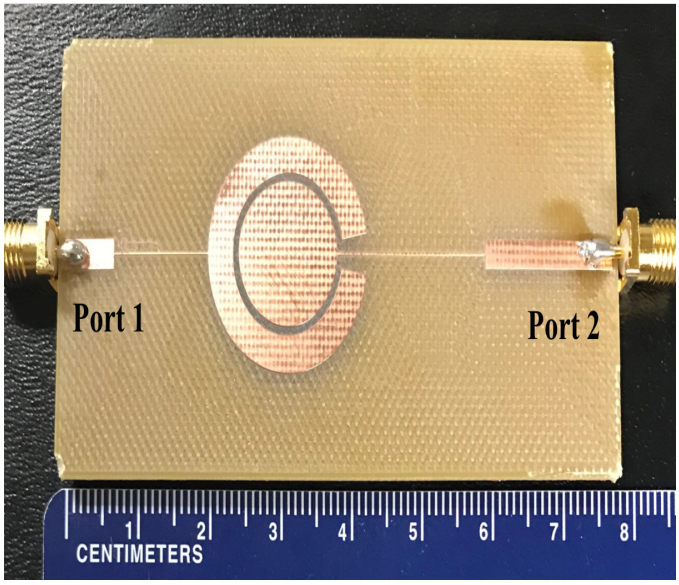

Figure 13: Photograph of the hybrid-fed microstrip TM_{110} -TM_{210} antenna

It is evident that the measurement and simulation results are in good agreement, with minor variations due to fabrication errors. The analytically predicted resonance frequencies obtained from Eqs. (5.1)(5.2a) are also highlighted (stars) in Figure 14. Our measurement results confirm the resonant behaviors of the proposed hybrid-fed patch antenna, with a noticeable dip of S_{11} at 3 GHz (fundamental frequency) and a dip of S_{22} at 6 GHz (second harmonic).

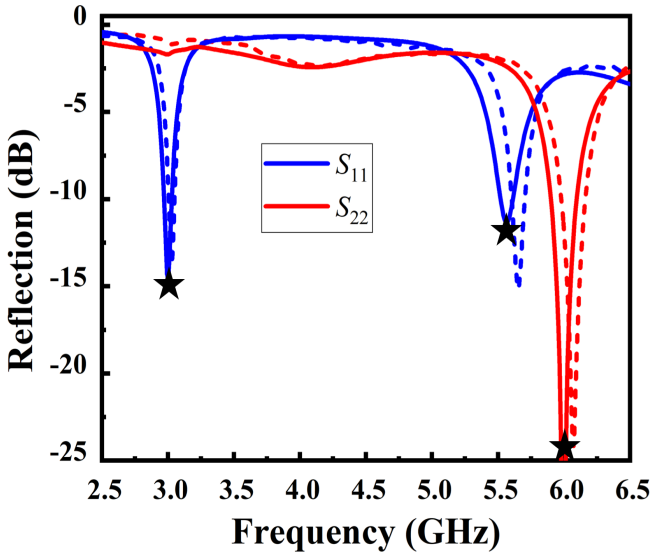

Figure 14: The simulated and measured reflection coefficient (S_{11} and S_{22}) of the antenna in 13

Moreover, both simulation and measurement results indicate good impedance matching. The -10 dB bandwidth is 50 MHz at 3 GHz and is 160 MHz at 6 GHz. There are also some higher-order modes excited in the inner circular patch (e.g., TM_{410} mode). However, the frequencies of these modes are far from the fundamental and second-harmonic frequencies, and should not affect the port isolation.

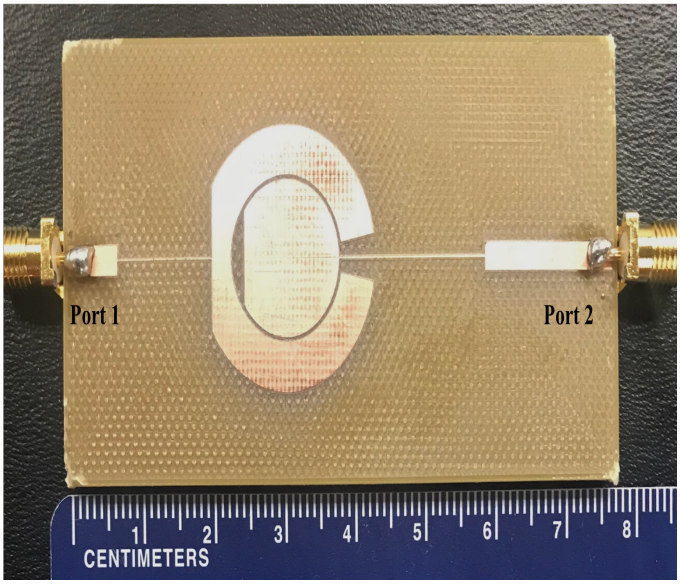

Figure 15: The hybrid-fed TM_{110}-TM_{210} microstrip antenna with modifying the radiation pattern

Although the proposed hybrid-fed microstrip antenna in figure 13 displays the desired operating frequencies, the radiation pattern is somewhat tilted due to the asymmetric current distributions, as the two feed lines could perturb the field distributions. To maximize the broadside radiation and achieve a more symmetric pattern, the patch geometry must be slightly modified. For instance, this task could be accomplished by introducing truncated corners.

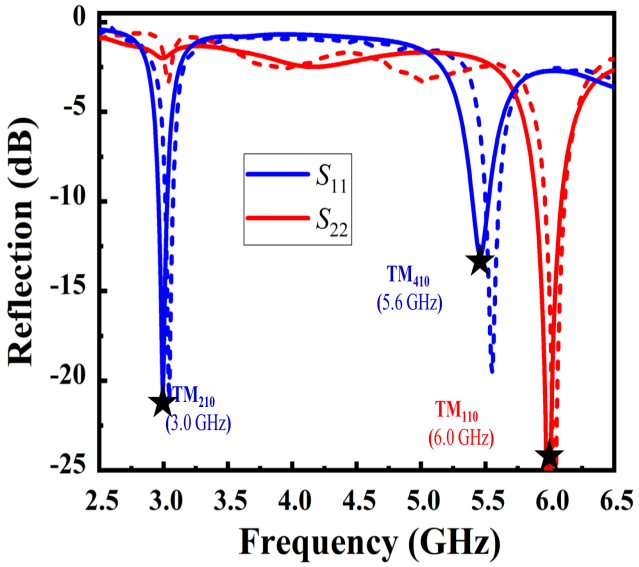

Figure 16: The simulated and measured reflection coefficient (S_{11} and S_{22}) of the antenna in 15

Figure 15 shows the optimum geometry of the hybrid-fed TM_{110}-TM_{210} microstrip antenna, whose structure is similar to figure 13, but with suitable geometric perturbations for modifying the radiation pattern. The geometric perturbation may not only enhance the broadside radiation pattern, but also improve the impedance matching and the realized gain. Figure 16 reports the simulated and measured reflection coefficients versus frequency, showing good isolation and impedance matching at the fundamental and second-harmonic frequencies. Figure 17 shows the simulated and measured radiation pattern at the operating frequencies,(a) and (b) are respectively the E-plane and H-plane radiation patterns at 3 GHz. (c) and (d) are respectively the E-plane and H-plane radiation patterns at 6 GHz.

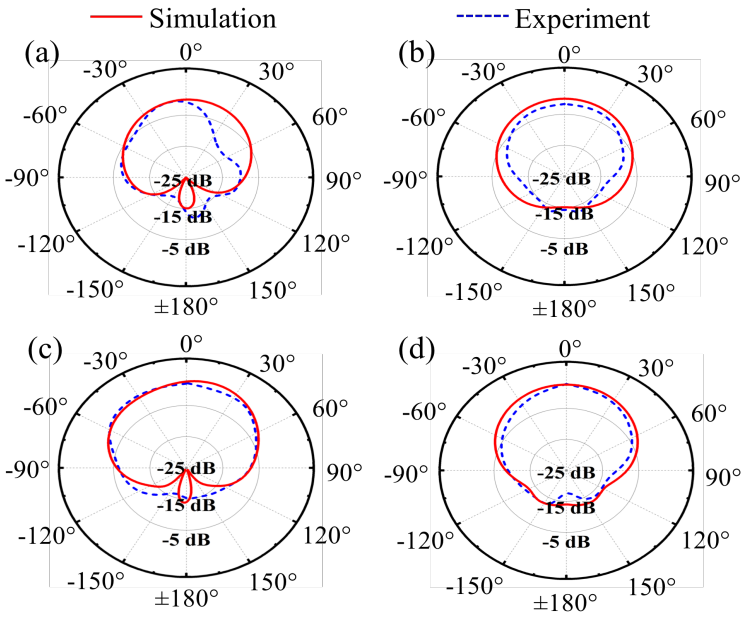

Figure 17: Simulated and measured radiation patterns for the modified hybrid-fed TM_{110}-TM_{210} antenna in figure 15

At 3 GHz (TM_{210} mode), this antenna exhibits a maximum realized gain of 1.03 dB, with a half-power beam width (HPBW) of 55°on the E-plane and a HPBW of 93°on H-plane. At 6 GHz (TM_{110} mode), this antenna exhibits a maximum gain of 2.83 dB, with a HPBW of 100°(74°) on the E-plane (H-plane). This hybridized TM_{110}-TM_{210} microstrip antenna may achieve considerable area and cost savings for the size-restricted harmonic transponders.

5.2.2 Hybrid-Fed TM_{110}-TM_{310} Microstrip Patch Antennas

Figures 18 and 19 show the fabricated TM_{110}-TM_{310} hybrid-fed microstrip antenna [figure 6(f)] and its measured reflection coefficients, respectively. It is clearly seen that the measurement results (dashed lines) agree quite well with the simulation results (solid lines), and the resonance frequencies can be quantitatively predicted by the analytical model (stars).We note that in this design, other higher-order modes, well predicted by Eqs. (5.1),(5.2a) and simulations, are excited in the split-ring patch antenna.

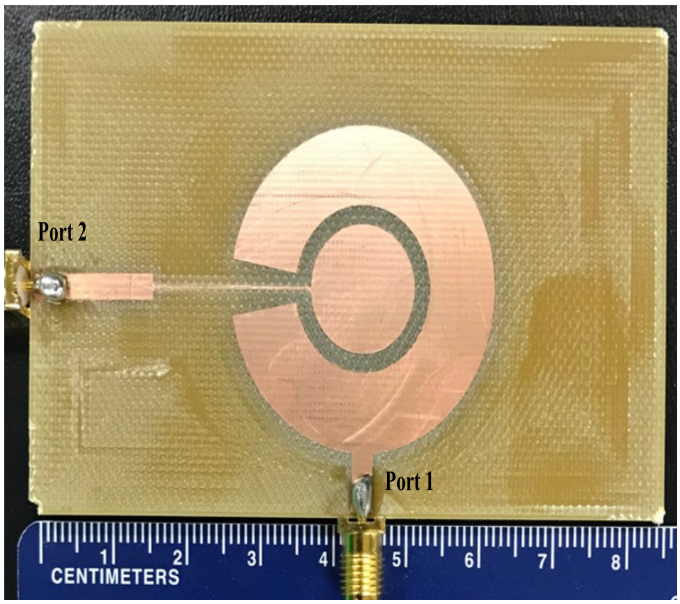

Figure 18: Photograph of the hybrid-fed microstrip TM_{110} - TM_{310} antenna

However, with properly designed patch geometry, good isolation and impedance matching can still be obtained, as can be seen in figure 19. There is no resonant mode overlapping with each other, particularly at the two frequencies of interest (3 GHz and 6 GHz). The measured -10 dB bandwidth is 50 MHz at 3 GHz and is 165 MHz at 6 GHz.

Also geometric perturbations is applied to the microstrip antenna in figure 18, aiming to enhance the directivity at the broadside and improve the symmetricity of radiation pattern.

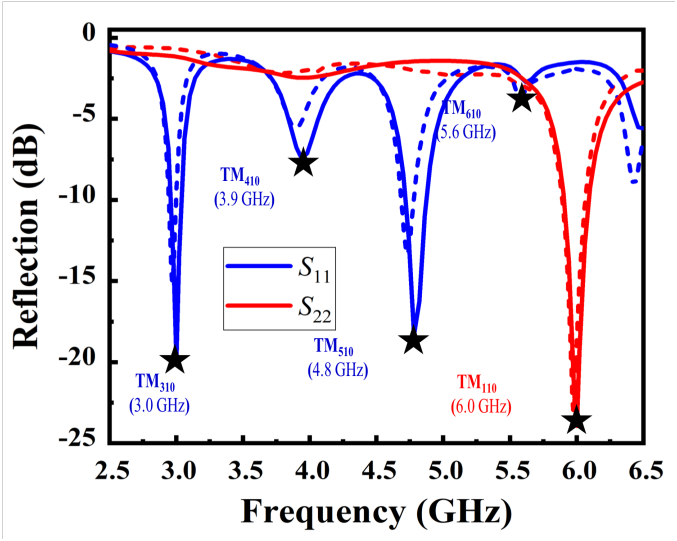

Figure 19: The simulated and measured reflection coefficient (S_{11} and S_{22}) of the antenna in 18

The optimized design is shown in figures 20 and 21 reports the simulated and measured reflection coefficients, showing excellent agreement for all resonant modes.

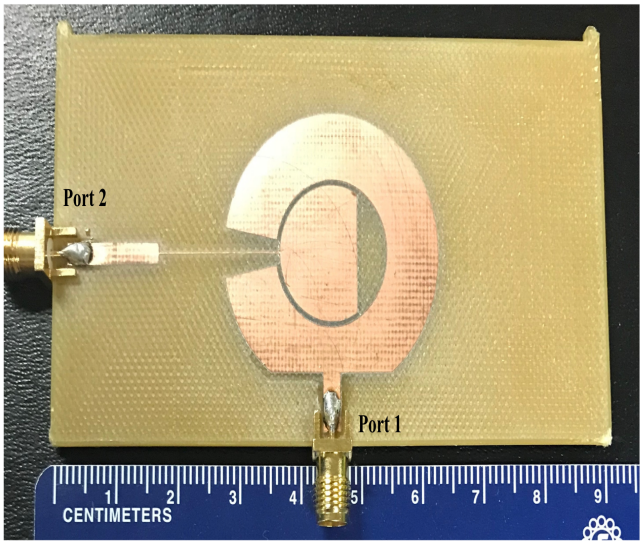

Figure 20: The hybrid-fed TM_{110}-TM_{310} microstrip antenna with modifying the radiation pattern

The measured -10 dB bandwidth is 50 MHz at 3 GHz and is 240 MHz at 6 GHz, which are nearly unchanged compared to those of the original design. Figure 22 shows the simulated and measured radiation patterns for the antenna in figure 20, where (a) and (b) are respectively the E-plane and H-plane radiation patterns at 3 GHz. (c) and (d) are respectively the E-plane and H-plane radiation patterns at 6 GHz.

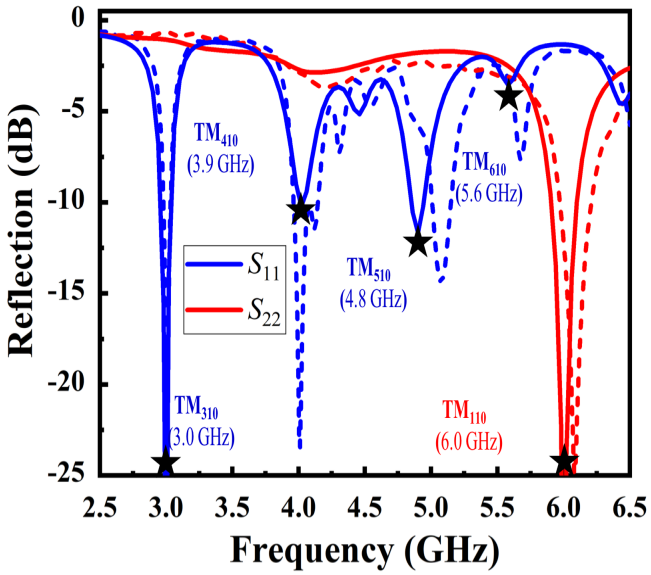

Figure 21: The simulated and measured reflection coefficient (S_{11} and S_{22}) of the antenna in 20

The measured maximum realized gain (TM_{310} mode) is 1.17 dB at 3 GHz, while the value is slightly improved to 3.33 dB at 6 GHz (TM_{110} mode). Compared to the hybrid-fed TM_{110}-TM_{210} microstrip antenna, although the total size of the hybrid-fed TM_{110}-TM_{310} microstrip antenna is somewhat increased, the distance between two feeding ports is reduced. Nonetheless, these two design alternatives have comparable matching and radiation performance, thus offering flexibility in the transponder integration among the antenna and electronic components (e.g., frequency doubler, matching circuit, and sensor).

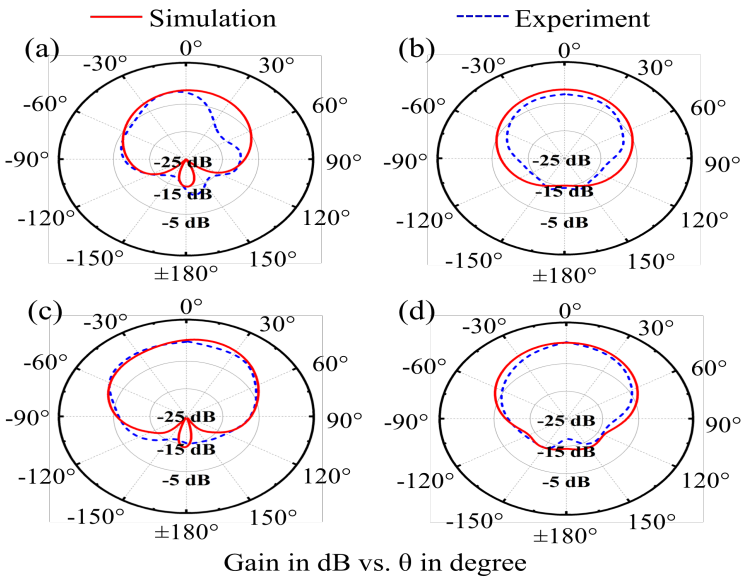

Figure 22: Simulated and measured radiation patterns for the modified hybrid-fed TM_{110}-TM_{310} antenna in figure 20.

we should note that due to relatively high dielectric and conduction losses, the measured radiation efficiencies of the above microstrip antennas are 40 % -70 % . The realized gain of the proposed antennas can be further enhanced by using a high-quality PCB substrate with low dissipation factors and by optimizing the shape of microstrip feeds.

6 HYBRID-FED AND ELLIPTICAL PATCH ANTENNA

Currently, micro-strip antennas, including hybrid-fed antenna and elliptical patch, are a preferred choice for most modern communication systems because they exhibit a low profile that is conformable to non-planar and planar surfaces. This chapter introduces hybrid-fed antenna and elliptical patch antenna.

An antenna characterizes a device that transmits and receives radio waves [49]. According to this definition, an antenna serves as a transitional device between a transmission line and free-space. The transmission line may be a waveguide or a coaxial line that transmits electromagnetic waves from the transmitter to the antenna or from the antenna to the receiving device. Other than transmitting and receiving electromagnetic energy, antennas are a sophisticated wireless system used in optimizing or accentuating the radiation energy in particular directions and suppressing it in others [49].

Therefore, an antenna serves as a probing and directional device. In wireless communication systems, an antenna serves as one of the most fundamental mechanism. A high-quality design of an antenna can improve system requirements and enhance general system performance. A contemporary example is a television for which the user can improve its general broadcast reception by using a high-performance antenna. In communication systems, antennas serve the same functions that eyes serve to animals. The field of antennas is wide and vigorous, and in the last 6 decades, technology has played a crucial role in the communications revolution. Most antenna improvements that emerged in this era are still in use today. However, numerous issues and challenges regarding their use have emerged because the demand for system performance is greater today than in the past. There are numerous types of antennas, including wire antennas, aperture antennas, micro-strip antennas, array antennas, reflector antennas, and lens antennas.

A micro-strip antenna comprises a dielectric material having a metallic pattern on its top side and a ground plane on its bottom side. Some of the common forms of micros-strip

antennas include a hybrid-fed antenna and elliptical patch antenna. These multifunctional antennas have become more significant today because of the speedy growth of modern wireless communications systems. Micro-strip antennas are a preferred choice for most modern communication systems because they exhibit a low profile that is conformable to non-planar and planar surfaces. Compared to other types of antenna, micro-strip antennas are also easy to fabricate using the printed circuit board technology. Additionally, they are mechanically strong when installed on rigid surfaces and are attuned with monolithic microwave integrated circuit (MMIC) designs. Specific micro-strip designs like elliptical patch antenna provide versatility in terms of polarizations, radiation patterns, impedances, and resonant frequencies.

In the 1970s and 1980s, applications of the hybrid-fed antenna and elliptical patch antenna in aviation industry became very popular [49]. Currently, they are used in numerous applications including government and commercial communication systems. They exist either in metallic, rectangular, or circular patches. Nevertheless, rectangular patches are very common, compared to the rests, because of their ease in fabrication, favorable radiation characteristics, and analysis. Designers consider micro-strip antennas to be low profile because they are conform-able to both non-planar and planar surfaces [49]. They are also easy and cost-effective to fabricate with the help of modern printed-circuit technology. They are mechanically strong and can be installed on inflexible surfaces, are well matched with MMIC design, and very adaptable in respect to polarization, patterns, impedance, and resonant frequencies. These antennas are usually installed on the surface of military aircraft, space satellites, spacecraft, cars, missiles, or handsets.

6.1 Hybrid-Fed Antenna

Researchers have undertaken numerous studies to increase the gain exhibited by micro-strip antennas [50]. In this attempt, they have employed numerous gain enhancing techniques. One of the major approaches of increasing antennas gain applies the array prin-

ciple. However, through this method, the complexity and the size of the circuit becomes a limitation. Therefore, researchers have been attempting to come up with better designs that will replace the use of array principle and keep the antenna sized as compact as possible. One of the most promising techniques has been the use of hybrid-fed configurations. Through this technique, several antennas are excited collectively under similar or dissimilar modes over an equal frequency range of operation.

Hybrid-fed antennas have a blend of series and parallel feeds. This feature enables a hybrid-fed antenna to attain a wider bandwidth compared with a series fed array with similar aperture size [50]. Due to the speedy advancement of modern communication systems, applications of hybrid-fed antennas have become very popular because they possess numerous radiation features. Moreover, hybrid-fed antennas provide promising solutions that can be developed to improve system performance by reducing multipath fading and improving channel capacity. These systems have diverse schemes that can be harnessed to boost the utility efficacy of the limited spatial and spectra resources [50]. With low-cost of fabrication, its compact size, and flexible configuration, the hybrid-fed antenna provides numerous opportunities for modern mobile communication systems.

Several ways of fabricating hybrid fed antennas exist. Using circular waveguide elements, one can join the circular apertures electromagnetically to a strip-line [50]. Through this, the overall radiation fuses to become a combination from both the open-ended and the strip line, enhancing the antenna's gain. Another technology utilizes a dipole and a rectangular patch antenna enclosed within a resonating ring to excite a surface mounted with a pyramidal horn [50]. In a different approach, a horn antenna is fed with stacked patches. To improve the general antenna efficiency, one has to replace the micro-strip patch antenna with a rectangular DRA.

Generally, a hybrid fed antennas represent a type of antenna system comprising an electronically scanned array integrated with radiating aperture [50]. These types of antennas

would be redundant if antenna engineers could design inexpensive phase arrays. In the future, if system designers create a cost-effective array that accommodates thousands of little components, it would be needleless to continue with the production of hybrid fed antennas [50]. Currently, phased array antennas are very expensive, making the production and applications of hybrid fed antennas to be among the most significant and most quickly developing technology in the field of antennas.

The basic hybrid-fed antenna comprises a radiating aperture integrated with a phased array. The radiating aperture is also referred to as objective aperture and may comprise of more structures such as sub-reflector, lens, or multiple-beam matrix [50]. Hybrid antennas have numerous applications in both military and civilian systems. These tasks relate to communication system applications because modern radars require speedy electronic beam agility. Hybrid-fed antennas with restricted sector coverage are applicable in fire control systems, weapon detectors, and traffic control systems. However, hybrid-fed antennas with very broad angular coverage are useful in strategic radar systems. Hybrid-fed antennas are also useful in non-scanning applications, such as systems fitted with feed devices for tolerance control in addition to jammer cancellation. Two types of hybrid fed antennas exist. They are a linearly polarized antenna and orthogonal linear polarized antenna [51].

6.1.1 The Linearly Polarized Hybrid Antenna

The linearly polarized hybrid antenna is a type of a hybrid antenna that integrates a circular-shaped dielectric resonator (DR) with an aperture-fed spherical micro-strip patch [51]. Unlike other hybrid-fed antennas, this antenna exhibits a directive radiation pattern. Additionally, its design process is simple, making it an attractive choice for numerous commercial applications. The dielectric resonator is fed by a spherical micro-strip patched on a slim grounded dielectric coating containing a low permittivity. The patch element is fed by a resonant gap on the ground surface by a 50 Ω micro-strip line edged on the rear of a second thin dielectric coating, which has a higher permittivity [51]. The differences

in permittivity guarantee that the feed line value always remains lesser than the patch, widespread issues experienced at the millimeter-wave frequency.

The design process of a linearly polarized hybrid antenna is comparatively simple. First, the system designer uses conventional methods to design an aperture coupled micro-strip patch that has no DR. Thereafter, the resonant frequency of TM_{110} mode is adjusted to cover the lower portion of the preferred impedance bandwidth [51]. To increase the resonance, the Lslot usually called the length of the slot, is roughly adjusted to half of the guided wavelength at a value just below the patch's resonant frequency. In this first step, the designer selects the width of the slot and other significant dimensions according to the performance of the selected PCB fabrication process.

To design the linearly polarized hybrid antenna described by Perron et al. a minimum width 0.15240 mm (6 mils) is acceptable. Concerning its DR with a HEM1nδ (where n = 1, 3, 5 ...), the designer should first select a hybrid mode and set it at its resonant frequency to cover the upper portion of the preferred band [51]. Perron et al claim that the field configurations exhibited by these families of hybrid modes are suitable for coupling with a micro-strip patch [51]. Nevertheless, Perron et al. warn that the designers should be careful when selecting the order n in the hybrid mode because it has a direct impact on the outline of the antennas' far-field radiation pattern [51]. Perron et al. also caution that designers should consider fabrication limitations when using this model [51]. Another model, Cohn's model, can also be applied in developing the approximation of the resonant frequency in the HEMmnδ hybrid modes of a circular-shaped DR position on a thin coating of the grounded substrate, as shown in the following formula:

$$f_{mn\delta}(GHz) = \frac{c}{2\pi\sqrt{\varepsilon_{eff}}}\sqrt{\left(\frac{\chi_{mn}}{r_{out}}\right)^2 + \left(\frac{\delta\pi}{2h_{eff}}\right)^2} \tag{6.1}$$

Where “c represents the speed of light, χ_{mn} represents the zero of derivative J’m (χ_{mn}) = 0 of the Bessel function Jm(x) for odd values of n and the zero of Jm(χ_{mn}) = 0 of the same Bessel function for even values of ” [51]. Table 1 outlines χ_{mn} values for hybrid modes of HEM1nδ (n = 1 to 8):

Hybrid mode	**χmn**	**Hybrid mode**	**χmn**
HEM11δ	**1.84120**	**HEM15δ**	**8.53630**
HEM12δ	**3.83180**	**HEM16δ**	**10.1735**
HEM13δ	**5.33150**	**HEM17δ**	**11.7060**
HEM14δ	**7.01560**	**HEM18δ**	**13.3237**

Table 1: χmn values of for hybrid modes of HEM1nδ (n = 1 to 8)

The δ factor indicated in equation (1) characterizes a quantity varying between 0 and 1, and represents the value of half wavelength deviations of the field contained in the z-direction [51]. To calculate it, one must solve the following sequence of equations:

$$\beta \times 2h_{eff} = 2 \times \tan^{-1}\left(\frac{\alpha}{\beta}\right) \tag{6.2}$$

$$\alpha = \sqrt{\left(\frac{x_{mn}}{r_{out}}\right)^2 - K_0^2} \tag{6.3}$$

$$\beta = \sqrt{K_0^2 \times \varepsilon_{eff} - \left(\frac{x_{mn}}{r_{out}}\right)^2} \tag{6.4}$$

$$\delta = \beta \times \frac{2h_{eff}}{\pi} \tag{6.5}$$

Equation (2) is a priori in natures and it should be computed numerically with mathematical software like Matlab. Its effective permittivity and height are illustrated as:

$$h_{eff} = h_1 + h_2 \tag{6.6}$$

$$\varepsilon_{eff} = \frac{V_{total}}{\frac{V_{hole}}{\varepsilon_{air}} + \frac{V_{ring}}{\varepsilon_{r1}} + \frac{V_{substrate}}{\varepsilon_{r2}}} = \frac{r_{out}^2 \times h_{eff}}{\frac{r_{in}^2 \times h_1}{\varepsilon_{air}} + \frac{h_1(r_{out}^2 - r_{in}^2)}{\varepsilon_{r1}} + \frac{r_{out}^2 \times h_2}{\varepsilon_{r2}}} \tag{6.7}$$

Where "ε_{air} represents the permittivity of air ($\approx$ 1), Vhole represents the volume of the DR hole, Vring represents the volume of the dielectric ring itself (without the hole), Vsubstrate represents the volume of the dielectric layer directly underneath the DR, and Vtotal represents the sum of these three volume" [51].

Based on the above analysis, it is apparent that the linearly polarized hybrid antenna exhibits several desirable characteristics, making it an excellent choice for many millimeter-wave applications. Nevertheless, more researchers are necessary to find ways of increasing its gain and reduce sidelobe levels to improving its performance.

6.1.2 Dual-Polarized Hybrid Antenna

The second type of hybrid-fed antenna is the dual-polarized hybrid antenna. This type of antenna is applied in transmitting and receiving signals via two orthogonal linear polarizations fed by two independent ports. The design of this antenna exhibits a circular-shaped DR ($\varepsilon r = 10.20; tan\delta$ = 0.00230) fed by a square-shaped patch imprinted on a dielectric substrate with thickness of (0.254 mm; $\varepsilon r = 2.2; tan\delta$ = 0.001). Additionally, the patch is fed through a pair of orthogonally predisposed slots with equal scopes on the ground plane

via two 50 Ω micro-strip lines etched on the rear of a second substrate film with a thickness of (0.2540 mm; $\varepsilon r = 10.20; tan\delta$ = 0.0023).

The L-shaped designs of the coupling slots make certain the two ports produce similar theoretical return loss, such as equal impendence bandwidth. The T-shaped disposition may be applied in elevating the isolation; however, this will cause a difference in impedance bandwidth in both ports. This condition has also been reported in dual-polarized-fed antennas operating at a frequency of 2.45GHz.

Perron et al. have designed a prototype of a dual-polarized hybrid antenna. The prototype was constructed using "Rogers Corporation" high-frequency laminates, RT/Duroid [51]. Perron et al. cut the DR using a computer-aided Nd-Yag Q laser machine before bonding the substrate together using droplets of cyanoacrylate [51]. The final product was a dual-polarized hybrid antenna with a comparatively large ground plane with dimensions of (Lx = Ly = 30 mm) that was later used to mount a brass housing to accommodate two 1.850 mm connectors. Perron et al. used VNA to measure the S-parameters of the antenna. Because the brass support and the connectors are excluded in the simulation models, Perron et al.'s prototype exhibited some discrepancies compared to the simulated models [51]. Nevertheless, the design exhibited impedance bandwidth (VSWR < 2) in both ports that were nearly similar to those of the simulated models.

Since the bandwidth of the dual-polarized hybrid antenna is comparatively large, over 8 GHz, oscillations within the measured curves are visible. This incidence is caused by the inductive loading effect occurring during the coaxial to micro-strip transition. In Perron et al.'s design, the recorded isolation was better than anticipated, it maintains over 20 dB across its bandwidth [51]. Applying a three-antenna technique, one can measure the dual-polarized hybrid antenna's gain for both polarizations. This will reveal two sets of results, representing the gain value when DR is in place and when DR is absent. In the prototypes, alignment errors may be introduced during the fabrication process. Similarly, connectors

may introduce transition losses during the assembling process.

Compared with linearly polarized hybrid antenna, the dual-polarized hybrid antenna has a higher gain value, with peak values of over 10 dB at around 56 GHz for both polarizations. The approximate simulated gain of a simple dual-polarized hybrid antenna is around 11.80 dB within the antenna's operational bandwidth [51]. This high-gain is attributed to an increase in radiator's electrical size whenever the DR is installed on its surface.

Another notable characteristic of the dual-polarized hybrid antenna is that on the radiation patterns its primary beam is directed towards the broadside. Similarly, its hybrid configurations are more directive compared to that of the micro-strip patch antenna. Dual-polarized hybrid antenna's radiation patterns also exhibit small side lobes at angles of 75°and 285°on the E-plane of its hybrid configuration. The side lobes are caused by the excitations of higher order hybrid modes within the DR of (the HEM13δ mode) [51]. Thus, by analyzing the electromagnetic distribution within a circular-shaped DR, one will realize that the circular-shaped DR serves as a dielectric waveguide, which distributes electromagnetic waves throughout its large aperture size. Undesirably, with an increase in frequency, the side lobes increases and gain reduces.

Like the linearly polarized hybrid antenna, the dual-polarized hybrid antenna has numerous desirable attributes, making it an excellent choice for many millimeter-wave applications. However, more researchers are necessary to find ways of increasing its gain and reduce sidelobe levels to improving its performance.

6.2 Elliptical Patch Antenna

Patch antennas represent types of an antenna classified as a low profile that can be installed on flat surfaces. It comprises a flat rectangular or square sheet called "patch" stacked on another bigger sheet denoted as a ground plane [52]. In modern wireless communication systems, patch antennas are very important because of they printable directly onto the circuit board. Additionally, they are very easy to fabricate and have a low profile that facilitates widespread application within the mobile phone market [52]. The radiation mechanism of this antenna occurs because of the gaps at each abridged edge of a micro-strip transmission line. These radiation makes the antenna to behave slightly larger electrically compared to its physical proportions. Thus, for the antenna to be at resonant, the designers have to shorten the transmission line just below the one-half a wavelength of the frequency used. Researchers have established that elliptical shaped micro-strip antennas mounted on printed circuit boards (PCB) have the capacity to emit spherical polarized waves that need only one feed and their geometrical designs are simple and sufficient to allow intricate theoretical analysis [53].

In certain applications of communications systems, the apertures for some antenna carriers are required to be spherical. For instance, in ship-borne satellite communication systems, it is necessary for the antenna's aperture of the antenna to be elliptical or rectangular [52]. In such situations, the normal rotationally symmetric-reflector antenna is unsuitable, whereas the elliptical aperture antenna is an ideal choice. Additionally, some situations necessitate an elliptical antenna. For example, in several satellite settings, the preferred ground coverage should be elliptical, necessitating the use of an elliptical beam antenna. Therefore, the applications of the elliptical antenna are becoming more popular in the field of radio engineering.

6.2.1 Circular Polarization

Polarization is a significant aspect when propagating signals between transmitting antenna and receiving antenna. The polarization plane denotes the level surface having the magnetic and electric field vectors and it is at all times in a perpendicular position to the plane of propagation. In an elliptical patch antenna, the contour outlined by the tilt of the electric field vector indicates the wave polarization. The contour appears in an ellipse outline. Its polarization direction is presumed to be in the direction of the major beam except when otherwise stated [54]. Currently, circular polarization is very significant in the field of antennas because it reduces the significance of antenna orientation with respect to the plane vertical to the direction of propagation [54]. Moreover, it provides much more suppleness to the angle between receiving and transmitting in addition to improving weather penetration and mobility.

6.2.2 Parameter Analysis Of Elliptical Patch Using Different Feeding Techniques

When designing an elliptical patch antenna, the designer has several options regarding the configurations used in feeding the antennas. Bansal and Gupta (2018) outlined the most popular approaches used in feeding techniques aimed at exciting elliptical patch antennas, comprising "micro-strip line, coaxial probe, aperture coupling, and proximity coupling" [54]. The analysis revealed that both the probe feed and micro-strip feed line configurations have intrinsic asymmetries that produce higher order modes, creating cross-polarized radiation. To overcome this challenge, aperture coupling is used. However, this methodology is the hardest to implement among the four techniques. Another disadvantage of aperture coupling is that it possesses a narrow bandwidth.

6.2.3 Analytical Advantages of Elliptical Patch Antenna

Compared with other types of micro-strip antennas, the elliptical patch antenna is the least reviewed because its geometry involves complex and higher mathematics. The theoretical handling of this type of antenna has been tried using numerous numerical pro-

cesses [54]. Through these techniques, it has been proved that elliptical shape provides some advantages, such as offering more degrees of flexibility and freedom in its design compared to the circular geometry.

One of the major benefits associated with elliptical patch antenna is circular polarization. This phenomenon is generated by exciting the elliptical patch using an appropriate choice of feed position at the ellipse. To create a circular polarization, a feed point ought to be positioned on the radial line comparatively with the major axis [54]. Additionally, the elliptic antenna provides more flexibility in the design because it uses the eccentricity and the focal length to calibrate the antenna into the preferred performance mode.

6.2.4 Modal Field Analysis of an Elliptical Patch Antenna

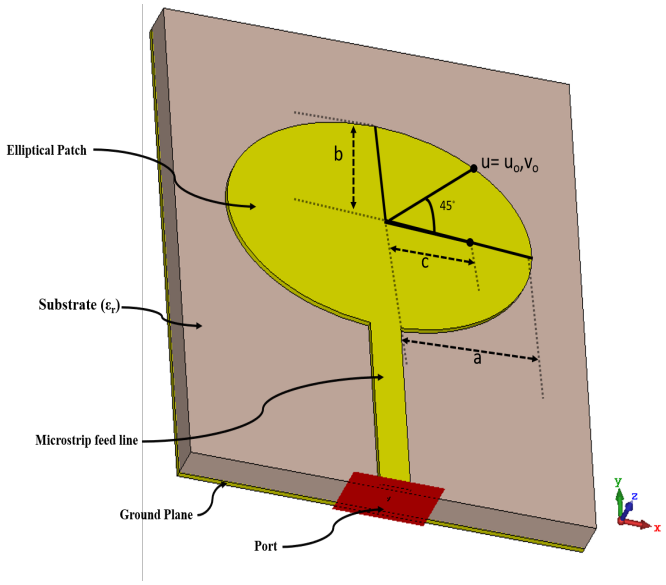

Figure 23: The geometry of an elliptical patch antenn

Figure 23 illustrates an elliptical micro-strip antenna having both semi-major axis and semi-minor axis lengths represented as “a” and “b” respectively. In its design, the thickness of the dielectric substrate’s thickness h is much smaller likened the excitation frequency’s free space wavelength, X [49]. Therefore, the foci of an elliptical patch antenna are situated at x = ± c, where:

$$c = \sqrt{a^2 - b^2} \tag{6.8}$$

Its rectangular coordinates (x,y) can be related to its elliptical co-ordinates (u, v) by use of the following equations:

$$x = c\ cosh\ u\ cos\ v, \tag{6.9}$$

$$y = c\ sinh\ u\ sin\ v. \tag{6.10}$$

A line current I_0 excites the elliptical antenna along the z-direction using the probe that serves as the primary conductor to the coaxial line fed from beneath the ground plane [49]. Notably, the excitation probe lies at a spot defined using $u = u_0$ at the semi-major axis. Therefore, an elliptical patch can be illustrated using:

$$u = u_0 = ln\Big(\frac{a+b}{c}\Big), \tag{6.11}$$

$$v_0 = tan^{-1}\Big(\frac{tan\ \phi_0}{tanh\ u_0}\Big) \tag{6.12}$$

Based on these definitions, the eccentricity of the ellipse can be represented as:

$$e = \frac{c}{a} \tag{6.13}$$

Given that $t \ll \lambda$, the probe's excitation current is presumed to be unvarying at I_0 relative to z, and thus, assumed that the modals fields are constant in the z-direction. Additionally, no charge accumulation exists between the ground plane and its patch. Based on these conditions, the only non-zero elements are E_Z, H_u, and H_v that matches with the TM mode [49]. Thus, the area between the ground plane and the patch acts a cavity resonator having plane spherical electric walls on its top and bottom sides and a spherical magnetic wall at its edges, as shown in figure 24:

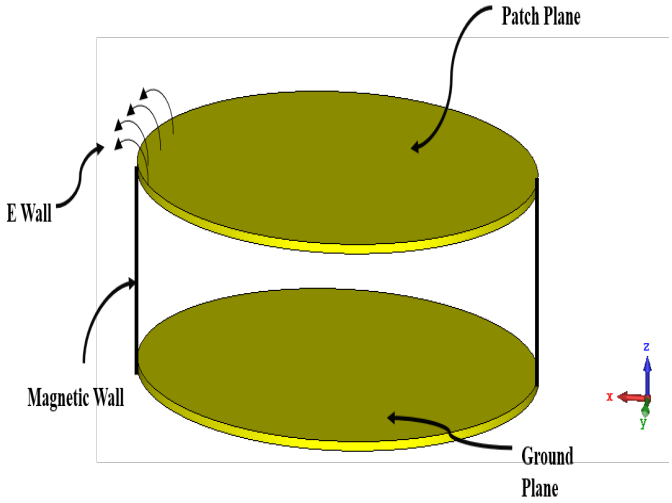

Figure 24: Cavity model of an elliptical patch antenna

Inside the cavity, the resonant modes are designated by TM_{nm} modes, where m and n denote deviations in the radial and azimuthal planes, respectively [49]. Thus, fields contained within the cavity meets the prerequisites of the wave equation:

$$\nabla^2 \bar{E} + k^2 \bar{E} = 0 \tag{6.14}$$

Regarding a thin substrate, in the z-direction, the field remains constant reducing equation (6.14) to

$$\frac{\partial^2 E_z}{\partial u^2} + \frac{\partial^2 E_z}{\partial v^2} + k^2 c^2 (cosh^2\ u - cos^2\ v) E_z = 0 \tag{6.15}$$

Within the elliptical coordinates, where

$$k = \omega \sqrt{u_0 \varepsilon_r} \tag{6.16}$$

ε_r and U_0 represent the dielectric substrates' relative permittivity and permeability re-

spectively. C is illustrated by equation (6.9) [49]. Therefore, the resultant field components with respect to E_Z are:

$$H_u = \frac{j}{\omega u_0 c} \frac{1}{\sqrt{cosh^2\ u - cos^2\ v}} \frac{\partial^2 E_z}{\partial v^2}, \tag{6.17}$$

$$H_v = \frac{j}{\omega u_0 c} \frac{1}{\sqrt{cosh^2\ u - cos^2\ v}} \frac{\partial^2 E_z}{\partial u^2} \tag{6.18}$$

Equation depicting the differential solution of equation (6.15) may be defined using even and odd n^{th} order of Mathieu's functions, indicated as:

$$E_z = \sum_{n=0}^{\infty} [\mathrm{A}_n So_n(h_{nmo,} \cos v) Jo_n(h_{nmo,} \cosh u) + B_n Se_n(h_{nme,} \cosh u)] \tag{6.19}$$

Where Jo_n (h_{nmo}, cosh u) and Je_n(h_{nmo}, cosh u) denote the radial Mathieu's functions and So_n(h_{nmo}, cos v) and Se_n (h_{nmo},cos v) represents the angular Mathieu's functions [49]. A_n and B_n denote constant variables.

$$A_n = \frac{-j\omega u_0 I_0 So_n(h_{nmo}, cos\ v)/M_n^o}{\left.\frac{\partial Jo_n(h_{nmo}, cosh\ u)}{\partial u}\right|_{u=u0} + jY_s \omega u_0 c \sqrt{cosh^2 u_0 - cos^2} Jo_n(h_{nmo}, cosh\ u)}, \tag{6.20}$$

$$B_n = \frac{-j\omega u_0 I_0 Se_n(h_{nmo}, cos\ v)/M_n^e}{\left.\frac{\partial Je_n(h_{nmo}, cosh\ u)}{\partial u}\right|_{u=u0} + jY_s \omega u_0 c \sqrt{cosh^2 u_0 - cos^2} Je_n(h_{nmo}, cosh\ u)}, \tag{6.21}$$

with

$$M_n^o = \int_0^{2\pi} [So_n(h_{nmo}, cos\ v)]^2 dv, \tag{6.22}$$

$$M_n^e = \int_0^{2\pi} [So_e(h_{nmo}, cos\ v)]^2 dv, \tag{6.23}$$

Where Y_s denotes the elliptical patch's surface admittance [49].

6.2.5 Analysis Of Elliptical Antenna Using The Cavity Model

Using the cavity model one can undertake an analysis of the operation of an elliptical micro-strip antenna [55]. To achieve this goal, one should compute the resonant frequencies of leading higher modes. Thereafter, the modal filed patterns' distribution for numerous modes should be, schemed. Using fringing aperture fields, the radiated fields are computed presuming that ideal magnetic walls exist at the periphery and on the electric walls on top and bottom of the antenna [55]. However, because the real fringing field distributions at the periphery are unknown, the designer should assume a consistent fringing field exist in the radial direction towards the width that is equivalent to the substrate thickness ($t \ll \lambda$) from its edges [55]. Radiated fields should also be established for the leading TMn mode having a design frequency of 3.20 GHz with out-of-band frequencies of 5.20, 7.20, and 9 GHz. Additionally, the radiation patterns are also computed for every higher order mode indicating the particular resonant frequency and respective out-of-band frequencies for both $\theta = 0^\circ$and $\theta = 90^\circ$ planes. All the patterns are standardized according to the E_0 component of the leading TMU mode.

In this analysis, a comprehensive assessment of the radiated fields generated using both in-band frequencies and out-of-band frequencies reveals that with an increase in the operating frequency a reduction in beam width is expected accompanied by an appearance of side lobes. On the $\theta = 0^\circ$ plane, the E_0 factor remains almost unchanged at both out-of-the band

and in-band frequencies [55]. On the $\theta = 90^{\circ}$ plane, both the E_0 and E_θ factors exhibit directional characteristics and the beamwidth of the E_0 factor reduces considerably.

In Nasimuddin (2015), a contrast between the investigational and theoretical results captured in literature matched [55]. They both showed that a rise in side lobe level and directivity results in an increase of out-of-band frequency. Given that both the TM_{31} and TM_{21} modes possess very low radiation amplitudes, the likelihood of interference signal merging at higher frequencies, out-of-band frequencies, is higher for the TM_{11} mode likened with other modes of operation [55]. Thus, out-of-band radiation properties of an elliptical patch antenna are helpful in estimating the electromagnetic interference that usually occurs in the main and the side lobes.

6.2.6 A Theoretical Analysis Of Elliptical Antenna Using Green'S Function Technique

It is commonly known that spherical polarized waves can be generated from elliptical patch antennas. Using Green's function technique to analyze an elliptical patch antenna, its modal fields, radiated fields, and input impedance expressions can be established. Mythili and Das (1999) undertook an experiment to establish the radiated field, modal field, and input impedance of an elliptical antenna [56]. They chose an antenna with dimensions of (a_1 = 1.450cm, b_1 = 1.340m, a_2 = 4cm, b_2 = 3.960cm, t = 0.1590cm and E = 2.55). They placed their feed at 2 cm away from the center of the antenna positioned at an angle of 45°with respect to the x-axis [56]. They calculated the resonant frequencies for numerous TM_{nm} modes (see table 2).

These resonant frequencies were used to establish current distribution patterns and modal field patterns for an elliptical antenna for its numerous TM_{nm} modes. The analysis of the patterns indicated far fields tallied and increased when the fringing fields in both the outer and inner edges pointed in the similar direction, resulting in utmost amplitude pointed at the boresight direction [56]. When both the outer and inner edges pointed in the different direction, it resulted in a subtracted amplitude that produced a null field pointed in the boresight direction.

Modes	Odd (GHz)	Even(GHz)
TM_{11}	1.1510	1.1230
TM_{12}	3.820	3.9400
TM_{13}	7.4490	7.6940
TM_{21}	2.1690	2.1450
TM_{22}	4.6340	4.7110
TM_{23}	7.8180	7.9850
TM_{31}	3.1070	3.0830
TM_{32}	5.5340	5.6300
TM_{33}	8.3250	8.4700

Table 2: Resonant frequencies of an elliptical antenna

This analysis also investigated the radiation patterns of numerous modes. The study revealed normalized radiated fields for the entire modes relative to "E_0 factors of the TM_{12} moderate in the $\theta = \pi/2$ plane" [56]. According to this illustration, the TM1n modes exhibit utmost radiation towards the boresight direction. The TM_{12} mode was the only mode that generated the highest maximum amplitude radiation at the middle point, characterized by two small side lobes. The analysis also indicated the effects of modes' negative interferences on the pattern of the fringing fields. This indicated that the width and the dielectric permittivity of the substrate affected the radiation outline of the TM_{12} mode. Thus, as ε_r reduces the main lobes together with the radiation amplitude increase, narrowing the beam width. Additionally, as the substrate's thickness t reduces, the main lobe's amplitude of the radiation pattern together with other side lobes increases [56]. These changes make the radiation pattern to be narrower and the nulls relocate into the center. Therefore, when fabricating an elliptical patch antenna the substrate's dielectric permittivity and its thickness should be redu enable narrowband applications.

6.2.7 Improving Radiation Performance Of An Elliptical Patch Antenna

One way of improving radiation performance of an elliptical patch antenna is to introduce sector slots in its design. Elliptical patch antenna can be modified by introducing two sector slots along its major axes line up opposite to each other another sector slot placed

aligned orthogonally to the two slots along the minor axis. In “Radiation Performance of an Elliptical Patch Antenna with Three Orthogonal Sector Slots”, Sharma and Saxena compared the radiation performance of conventional elliptical patch antenna and a modified antenna containing three orthogonal sector slots [57]. They optimized the location and magnitudes of these sector slots to realize an enhanced bandwidth that increased by around 10.96%. The increase is almost four times higher than that of the usual elliptical patch antenna excited under the same test conditions [57]. The researchers compared the experimental findings with simulation findings to enhanced understanding. The study outcomes revealed that the introduction of orthogonal sector slots reduces the effective patch size and improves the general performance of the antenna [57]. The modified patch antenna had increased gain and impedance bandwidth compared to that of a conventional antenna. An analysis of the modified antenna’s radiation pattern indicated stable outlines with maximum radiations at a normal direction to patch geometry. This he modified antenna satisfies the bandwidth standards stipulated by the IEEE for wireless local area network (WLAN) [57].

6.3 Microfluidic-Integrated, Dual-Resonant Elliptical Microstrip Antennas for Making Compact Harmonic-Transponder

In this section, I proposed a compact dual-resonant elliptical microstrip patch antenna, employing the even order TM_{c110} mode as fundamental tone receiver and the odd TM_{s110} mode as the second harmonic tone transmitter as depicted in Figure 25. Different from conventional harmonic tags using separate antennas at different frequencies, the proposed single-fed elliptical patch antenna can significantly reduce the area occupation and can be designed by an approximate analytical model.

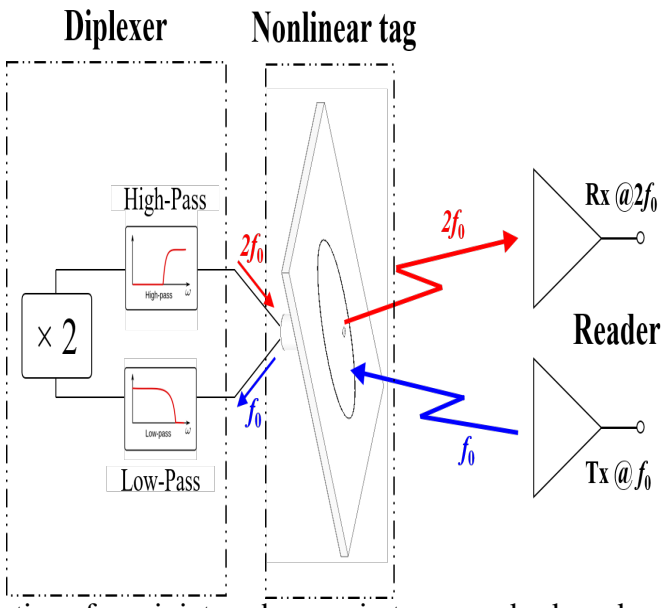

Figure 25: Schematics of a miniature harmonic transponder based on the proposed dual-resonant elliptical microstrip patch antenna

I design and experimentally validate a microfluidic-integrated, dual-resonant elliptical microstrip patch antenna, which can receive fundamental tone and re-transmit the second harmonic signal. The proposed elliptical harmonic transponder consists of an elliptical patch with two shorting pins precisely drilled through the substrate. The proposed antenna can operate in the even order TM_{c110} mode (fundamental frequency; 3 GHz) and the odd

order TM_{s110} mode (second harmonic frequency; 6 GHz). Moreover, analytical expressions were derived for calculating the elliptical microstrip antenna's resonant frequencies.

This section is organized as follows. In Section 6.3.1, I will first use the cavity model to predict resonant modes and electrical field distributions of the proposed antenna, which is important for providing theoretical basis for my elliptical antenna design. Then, I will conduct the full-wave simulation to verify analytical results. In Section 6.3.2, at first, I experimentally study the performance of the proposed dual-resonant elliptical patch antenna with two operating frequency at 3 GHz (fundamental tone) and 6 GHz (second harmonic tone) by characterizing its reflection coefficient, radiation efficiency, radiation pattern, and antenna gain.

6.3.1 Design and Simulation

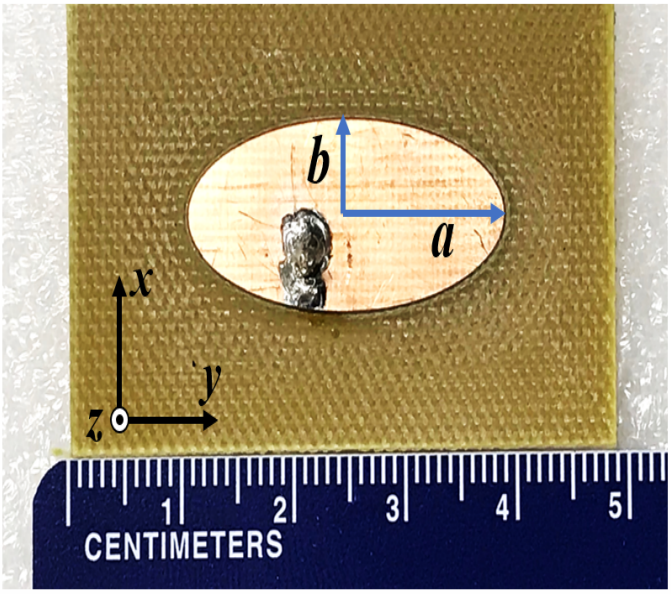

Figure 26: Photograph of the dual-resonant elliptical microstrip antenna

Figure 25 illustrates the geometry of the proposed dual-resonant elliptical microstrip antenna with the major and minor half-axis length a and b, as shown in Figure 26. The elliptical patch layer is separated from the ground plane by the FR4 substrate with relative permittivity ε_r = 4.25, loss tangent δ = 0.015, and thickness d = 1.5 mm. Since I assume the thickness of the substrate is much smaller than the operating wavelength, the resonant frequencies of this dual-resonant elliptical antenna can be approximately estimated by using the standard cavity model [58] [59], where the major and minor half-axis of the ellipse resonates at the fundamental frequency (f_0) and at the second harmonic frequency ($2f_0$), respectively.

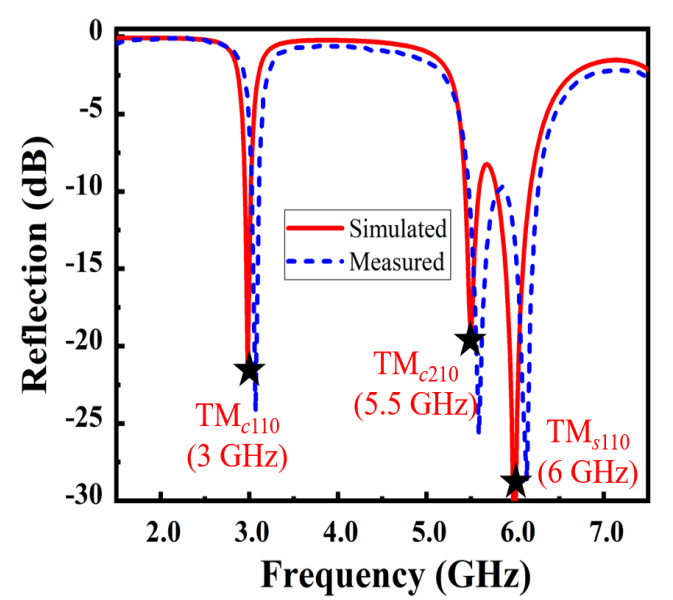

Figure 27: The simulated and measured reflection coefficient (S_{11}) of the antenna

In this elliptical cavity, the perfect electric conductor (PEC) boundary condition is applied at the top and bottom surfaces, and the perfect magnetic conductor (PMC) is assumed on sidewalls.

Here, I have conducted the full-wave numerical simulation based on the frequency-domain finite-element method to validate the resonant frequencies predicted by the cavity model. I have designed the compact dual-resonant elliptical patch antenna with the fundamental tone at 3 GHz and the second harmonic tone at 6 GHz with the geometry a = 14.4 mm and b = 6.336 mm. The eigenmodal analysis of the electric field distribution are shown in Figure 28(a)-(b), which not only confirm the accuracy of the theoretical cavity model, but also provide the guideline for choosing optimal feeding position.

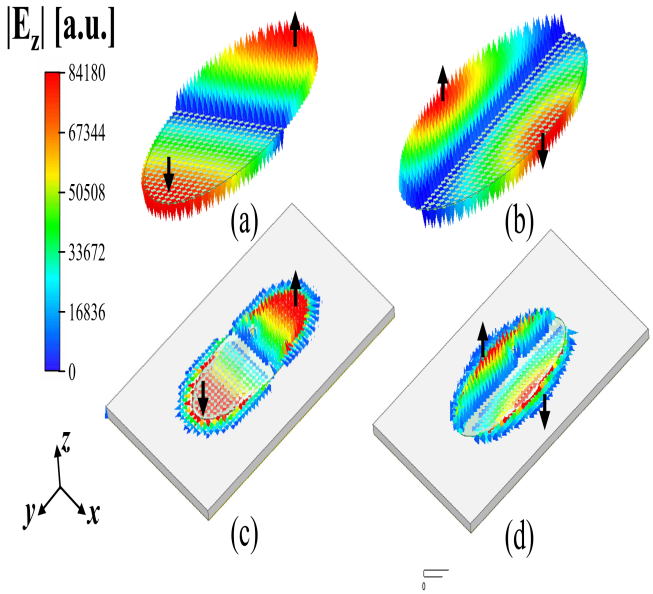

Figure 28: Electric Field (Ez) Distributions for the Elliptical Patch

The optimum positions of feed point for simultaneously exciting TM_{c110} mode and TM_{s110} mode can be obtained by observing the location of maximum field intensities in Figure 28(a) and 2(b). By utilizing rin = 0.635mm 50 ohms coaxial cable feed at position x = 3 mm and y = 3.5 mm, I can simultaneously excite even order TM_{c110} mode and odd order TM_{s110} mode with good impedance matching. The calculated snapshots of electric field distribution at the resonance frequency (which coincides with the analytical results) are presented in Figure 28. Here, I find a good agreement between the full-wave simulation results of the realistic dual-resonant elliptical patch antennas [Figure 28(c)-(d)] and those obtained from the eigenmodal analysis [Figure 28(a)-(b)]. Such results further demonstrate the effectiveness of my analytical approach.

6.3.2 Measurement Results

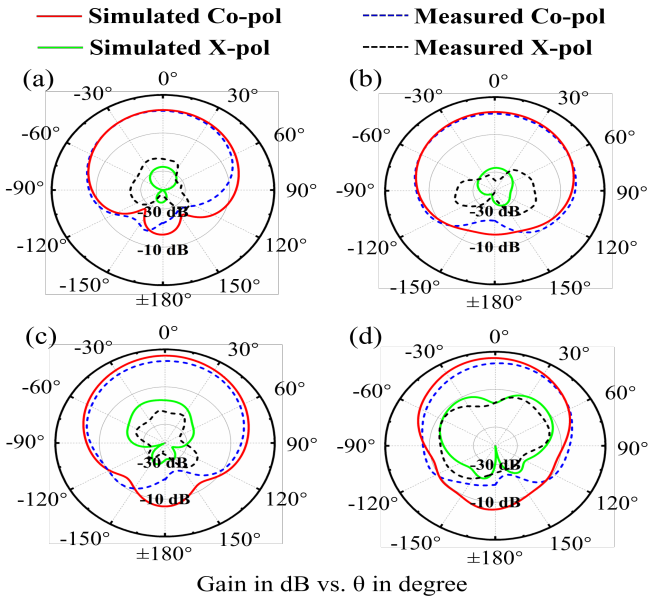

Figure 29: Simulated and measured radiation pattern for the dual-resonant elliptical antenna

I have fabricated the proposed microstrip antenna using the low-cost printed-circuit board (PCB) technique, with FR4 substrate and copper (Cu) microstrips. figure 25 shows the fabricated dual-resonant elliptical microstrip antenna analyzed in figure 28; here, I directly use single 50 ohms coaxial cable feed method to excite fundamental tone TM_{c110} mode and the second harmonic TM_{s110} mode at the same time. For the harmonic transponder design, the fundamental tone will be received by the major axis of the elliptical patch and be guided to the port which is connected to a diplexer to double the frequency, and then the frequency-doubled RF signal will be re-guided through the same port and re-radiate through the minor axis. Figure 27 reports the simulated (solid lines) and measured (dashed lines) reflection coefficients, S_{11}, versus frequency for the microstrip antenna in figure 26. It is evident that the measurement and simulation results are in good agreement, with minor variations due to the fabrication errors or the fluctuations of the substrate permittivity. The analytically predicted resonance frequencies including even order TM_{c210} mode obtained

are also highlighted (stars) in figure 27. my measurement results confirm the dual-resonant behaviors of my proposed dual-resonant elliptical microstrip antenna, with a noticeable dip at 3 GHz (fundamental frequency) and at 6 GHz (second harmonic). Moreover, both simulation and measurement results indicate good impedance matching simultaneously. The -10 dB measured impedance bandwidth is 80 MHz at 3.07 GHz and is 350 MHz at 6.13 GHz, which is closed to the simulated result 70 MHz at 3 GHz and is 380 MHz at 6 GHz. figure 29 shows the simulated and measured radiation pattern of the proposed antenna on the E-plane and H-plane at two operating frequencies, 3 GHz and 6 GHz. It is evident seen that the measured co-polarization radiation pattern with broadside radiation feature is in good agreement with the simulated one. At 3 GHz (TM_{c110} mode), this antenna exhibits a maximum realized gain of 2.66 dB, with a half-power beamwidth (HPBW) of 92°on the E-plane and a HPBW of 106°on H-plane. At 6 GHz (TM_{s110} mode), this antenna exhibits a maximum gain of 4.84 dB, with a HPBW of 84°(66°) on the E-plane (H-plane). Moreover, the measured cross-polarization radiation pattern is less than -20 dB (-10 dB) on the E-plane (H-plane). I should note that due to relatively high dielectric and conduction losses, the measured radiation efficiencies of the above-mentioned microstrip antennas are 45% at 3 GHz and 83% at 6 GHz. The realized gain of the proposed antennas can be further enhanced by using a high-quality PCB substrate with low dissipation factors.

7 CONCLUSION AND FUTURE WORK

7.1 Conclusion

Compact and low-cost dual-resonance microstrip patch antennas are of particular interest for applications in harmonics-based nonlinear radar and sensing systems. Harmonic radar or harmonic sensor can signifyingly suppress the clutters, echoes, electromagnetic interferences and cross talks, thus enabling a great signal-to-noise ratio (SNR). Here, I have proposed new types of conformal and low-profile microstrip patch antennas for making small-size harmonic transponders. These antennas have isolated resonances at the fundamental and second-harmonic frequencies that can be fully modeled by my analytical solution. In addition, they adopt the hybrid-fed structures with two ports matched to the input and output of the frequency multiplier or sensor. This helps saving not only the total size of antenna, but also at least one stage of filter, matching network or signal diplexer.

In this thesis, I report two types of hybrid-fed patch antennas, which exhibit two orthogonal (linear) polarization at the fundamental and second-harmonic frequencies. In this first design, I have demonstrated that the TM_{110} and TM_{210} (or TM_{310}) modes can be respectively excited at 3 GHz and 6 GHz by tailoring positions of the feed point and the geometry of hybridized C-ring/circular patch antenna. The measurement results show a satisfactory antenna gain with broadside radiation patterns, good impedance matching and good port isolation.

In the second design, I propose a hybrid-coaxial-fed elliptical patch antenna. Another advantage of using elliptical patch antenna is that provides more flexibility in its design because it uses the eccentricity and the focal length to calibrate the antenna into the preferred performance mode. Specifically, I have designed a patch antenna that can excite the fundamental odd and even modes at the two desired frequencies, while suppressing the higher-order modes by properly loading the shorting-pin. The proposed microstrip antennas may benefit various many size-restricted harmonic transponders used for harmonic

radars, harmonic sensors, medical implants, passive radio-frequency identification (RFID), and internet-of-things (IoT) applications.

7.2 Future Work

I advise the design of the Frequency Doubler, Pass Band Filter and the Amplifier for future work for completing the Harmonic Radar System. I will recommend the Frequency Doubler; a system of two components where one part performs the multiplication of the fundamental frequency, and the other converts input power frequency to match the designed harmonic frequency. The design is planned to begin from the fundamental optimization of broad bandwidth and the system's efficiency based on the current antenna design and the radar performance constraints.

For band-pass filter design, I would recommend the filter's DR as the resonant frequency for the given voltage length and assumed the maximum coupling factors between the micro-strip and the DR (βi). I Suggest employing the Gómez (36) principle to design the frequency response for the temperature sensing system. Also, bandpass bandwidth will be given by the final frequency due to a change in temperature less initial frequency. I further Suggest using the Gómez (37) formulation to design the coupling efficiency where the dissipated power is measured by the transmitted and reflected radiation in reference to the input oscillation.

The design will also include the Power and Low-Noise Amplifiers. Both cases will entail the definition of the load impedance that gives the maximum power, bridging-gap and the coefficient of the gain compression. I also Recommend to specify the pad ground inductance and Mu-Factor to establish the amplification stability. Additionally, I will adopt Smith Chart Utility to study the system frequency response, view the coordination of network design component and network topology. I also intend to employ ADS Momentum and Momentum Components approach to analyze the impact of physical layout parasitic on the efficiency and application of the amplifiers.

REFERENCE

[1] J. Zhang, G. Y. Tian, A. M. Marindra, A. I. Sunny, and A. B. Zhao, "A review of passive rfid tag antenna-based sensors and systems for structural health monitoring applications," *Sensors*, vol. 17, no. 2, p. 265, 2017.

[2] S. Amendola, R. Lodato, S. Manzari, C. Occhiuzzi, and G. Marrocco, "Rfid technology for iot-based personal healthcare in smart spaces," *IEEE Internet of things journal*, vol. 1, no. 2, pp. 144–152, 2014.

[3] J. Riley, A. Smith, D. Reynolds, A. Edwards, J. Osborne, I. Williams, N. Carreck, and G. Poppy, "Tracking bees with harmonic radar," *Nature*, vol. 379, no. 6560, p. 29, 1996.

[4] D. Psychoudakis, W. Moulder, C.-C. Chen, H. Zhu, and J. L. Volakis, "A portable low-power harmonic radar system and conformal tag for insect tracking," *IEEE Antennas and Wireless Propagation Letters*, vol. 7, pp. 444–447, 2008.

[5] H. Huang, L. Tao, F. Liu, L. Ji, Y. Hu, M. M.-C. Cheng, P.-Y. Chen, and D. Akinwande, "Chemical-sensitive graphene modulator with a memory effect for internet-of-things applications," *Microsystems & Nanoengineering*, vol. 2, p. 16018, 2016.

[6] A. Lazaro, R. Villarino, and D. Girbau, "A passive harmonic tag for humidity sensing," *International Journal of Antennas and Propagation*, vol. 2014, 2014.

[7] H. Huang, M. Sakhdari, M. Hajizadegan, A. Shahini, D. Akinwande, and P.-Y. Chen, "Toward transparent and self-activated graphene harmonic transponder sensors," *Applied Physics Letters*, vol. 108, no. 17, p. 173503, 2016.

[8] F. Alimenti and L. Roselli, "Theory of zero-power rfid sensors based on harmonic generation and orthogonally polarized antennas," *Progress In Electromagnetics Research*, vol. 134, pp. 337–357, 2013.

[9] K. Rasilainen, J. Ilvonen, A. Lehtovuori, J.-M. Hannula, and V. Viikari, "Harmonic transponders: Performance and challenges," *Progress In Electromagnetics Research M*, vol. 41, pp. 139–147, 2015.

[10] V. Palazzi, F. Alimenti, P. Mezzanotte, M. Virili, C. Mariotti, G. Orecchini, and L. Roselli, "Low-power frequency doubler in cellulose-based materials for harmonic rfid applications," *IEEE Microwave and Wireless Components Letters*, vol. 24, no. 12, pp. 896–898, 2014.

[11] D. MASCANZONI and H. WALLIN, "The harmonic radar: a new method of tracing insects in the field," *Ecological entomology*, vol. 11, no. 4, pp. 387–390, 1986.

[12] H. Huang, P.-Y. Chen, C.-H. Hung, R. Gharpurey, and D. Akinwande, "A zero power harmonic transponder sensor for ubiquitous wireless μl liquid-volume monitoring," *Scientific reports*, vol. 6, p. 18795, 2016.

[13] D. Ahbe, S. Beer, T. Zwick, Y. Wang, and M. M. Tentzeris, "Dual-band antennas for frequency-doubler-based wireless strain sensing," *IEEE Antennas and wireless propagation letters*, vol. 11, pp. 216–219, 2012.

[14] B. Kubina, J. Romeu, C. Mandel, M. Schüßler, and R. Jakoby, "Quasi-chipless wireless temperature sensor based on harmonic radar," *Electronics Letters*, vol. 50, no. 2, pp. 86–88, 2014.

[15] B. Kubina, C. Mandel, M. Schüßler, and R. Jakoby, "Compact quasi-chipless harmonic radar sensor with a dielectric resonator antenna," in *Microwave Symposium (IMS), 2015 IEEE MTT-S International*, pp. 1–3, IEEE, 2015.

[16] R. Brazee, E. Miller, M. Reding, M. Klein, B. Nudd, and H. Zhu, "A transponder for harmonic radar tracking of the black vine weevil in behavioral research," *Transactions of the ASAE*, vol. 48, no. 2, pp. 831–838, 2005.

[17] K. Rasilainen, J. Ilvonen, J.-M. Hannula, and V. Viikari, "Designing harmonic transponders using lumped-component matching circuits," *IEEE Antennas and Wireless Propagation Letters*, vol. 16, pp. 246–249, 2017.

[18] C. Mariotti, F. Alimenti, M. Virili, G. Orecchini, P. Mezzanotte, and L. Roselli, "Harmonic chipless sensor exploiting wireless autonomous communication and energy transfer," in *Wireless Power Transfer Conference (WPTC), 2014 IEEE*, pp. 24–27, IEEE, 2014.

[19] Z.-M. Tsai, P.-H. Jau, N.-C. Kuo, J.-C. Kao, K.-Y. Lin, F.-R. Chang, E.-C. Yang, and H. Wang, "A high-range-accuracy and high-sensitivity harmonic radar using pulse pseudorandom code for bee searching," *IEEE Transactions on Microwave Theory and Techniques*, vol. 61, no. 1, pp. 666–675, 2013.

[20] L. Agarwal and P. Rastogi, "Design and analysis of circularly polarized micro-strip patch antenna using hfss," *International Journal of Computer Applications*, vol. 124, no. 16, 2015.

[21] J. Landt, "The history of rfid," *IEEE potentials*, vol. 24, no. 4, pp. 8–11, 2005.

[22] R. Li, G. Dejean, M. M. Tentzeris, and J. Laskar, "Development of multi-broadband planar wire antennas for wireless applications," *Wireless Personal Communications*, vol. 42, no. 1, pp. 1–11, 2007.

[23] V. Kizimenko, "New broadband microstrip antenna design," in *Antenna Theory and Techniques (ICATT), 2011 VIII International Conference on*, pp. 153–155, IEEE, 2011.

[24] A. K. Bhattacharyya and R. Garg, "Analysis of annular sector and circular sector microstrip patch antennas," *Electromagnetics*, vol. 6, no. 3, pp. 229–242, 1986.

[25] E. Nishiyama, M. Aikawa, and S. Egashira, "Fdtd analysis of stacked microstrip antenna with high gain," *Progress In Electromagnetics Research*, vol. 33, pp. 29–43, 2001.

[26] J. Gomez-Tagle and C. G. Christodoulou, "Extended cavity model analysis of stacked microstrip ring antennas," *IEEE Transactions on Antennas and Propagation*, vol. 45, no. 11, pp. 1626–1635, 1997.

[27] J. Anguera, C. Puente, C. Borja, N. Delbene, and J. Soler, "Dual-frequency broadband stacked microstrip patch antenna," *IEEE Antennas and Wireless Propagation Letters*, vol. 2, no. 1, pp. 36–39, 2003.

[28] T. Chakravarty, S. M. Roy, S. K. Sanyal, and A. De, "A novel microstrip patch antenna with large impedance bandwidth in vhf/uhf rang," *Progress In Electromagnetics Research*, vol. 54, pp. 83–93, 2005.

[29] S. M. Presas, "Microwave frequency doubler integrated with miniaturized planar antennas," 2008.

[30] "Matlab optimization toolbox."

[31] D.-G. Fang, *Antenna theory and microstrip antennas*. CRC Press, 2009.

[32] J. R. Patel and J. B. Chaudhari, "Optimization and return loss reduction of microstrip patch antenna," *International Journal of Innovative Research in Computer and Communication Engineering*, vol. 3, no. 6, pp. 4996–5003, 2015.

[33] T. S. Bird, "Definition and misuse of return loss [report of the transactions editor-in-chief]," *IEEE Antennas and Propagation Magazine*, vol. 51, no. 2, pp. 166–167, 2009.

[34] A. Eroglu, *RF circuit design techniques for MF-UHF applications*. CRC press, 2013.

[35] A. Tulintseff and R. Sorbello, "Current and radiation fields of electromagnetically coupled microstrip antennas," in *Antennas and Propagation Society International Symposium, 1987*, vol. 25, pp. 928–931, IEEE, 1987.

[36] S. Hardiati, "Aplikasi substrat alumina pada antena mikrostrip patch persegi untuk komunikasi bergerak pada frekuensi (3, 3-3, 4) ghz," in *Industrial Electronic Seminar*, 2010.

[37] A. El Alami, S. D. Bennani, M. El Bekkali, and A. Benbassou, "Modeling the radiation characteristics of a circular patch antenna by using cavity model for rfid applications," *European Journal of Scientific Research*, vol. 110, no. 1, pp. 199–207, 2013.

[38] Z. Fan and K.-F. Lee, "Hankel transform domain analysis of dual-frequency stacked circular-disk and annular-ring microstrip antennas," *IEEE Transactions on Antennas and Propagation*, vol. 39, no. 6, pp. 867–870, 1991.

[39] R. Cock and C. Christodoulou, "Design of a two-layer, capacitively coupled, microstrip patch antenna element for broadband applications," in *Antennas and Propagation Society International Symposium, 1987*, vol. 25, pp. 936–939, IEEE, 1987.

[40] G. Brooker, *Introduction to sensors for ranging and imaging*. The Institution of Engineering and Technology, 2009.

[41] J. Lao, R. Jin, J. Geng, and Q. Wu, "An ultra-wideband microstrip elliptical slot antenna excited by a circular patch," *Microwave and Optical Technology Letters*, vol. 50, no. 4, pp. 845–846, 2008.

[42] N. C. Azenui and H. Yang, "A printed crescent patch antenna for ultrawideband applications," *IEEE Antennas and Wireless Propagation Letters*, vol. 6, pp. 113–116, 2007.

[43] P. H. Vardhini and N. Koteswaramma, "Patch antenna design with fr-4 epoxy substrate for multiband wireless communications using cst microwave studio," in *Electrical, Electronics, and Optimization Techniques (ICEEOT), International Conference on*, pp. 1811–1815, IEEE, 2016.

[44] F. Hirtenfelder, "Effective antenna simulations using cst microwave studio®," in *Antennas, 2007. INICA'07. 2nd International ITG Conference on*, pp. 239–239, IEEE, 2007.

[45] M. Scarpino, *Designing Circuit Boards with EAGLE: Make High-quality PCBs at Low Cost*. Pearson Education, 2014.

[46] S. Monk and D. Amos, *Make Your Own PCBs with EAGLE: From Schematic Designs to Finished Boards*. McGraw-Hill Education, 2014.

[47] X. Jia, Q. Feng, T. Fan, and Q. Lei, "Rfid technology and its applications in internet of things (iot)," in *Consumer Electronics, Communications and Networks (CECNet), 2012 2nd International Conference on*, pp. 1282–1285, IEEE, 2012.

[48] M. Studio, "Cst-computer simulation technology," *Bad Nuheimer Str*, vol. 19, p. 64289, 2008.

[49] A. B. Constantine *et al.*, "Antenna theory: analysis and design," *MICROSTRIP ANTENNAS, fourth edition, John wiley & sons*, 2016.

[50] A. W. Rudge, K. Milne, and A. D. Olver, *The handbook of antenna design*, vol. 16. IET, 1982.

[51] A. Perron, A. Sebak, and T. Denidni, *Hybrid Microstrip Antennas*. INTECH Open Access Publisher, 2011.

[52] M. Jamlos, R. Rahim, H. Othman, M. Jusoh, Z. Ahmad, M. Romli, and M. Salimi, "2.45 ghz of elliptical shape patch antenna," in *Wireless Technology and Applications (ISWTA), 2012 IEEE Symposium on*, pp. 126–129, IEEE, 2012.

[53] K. Wei, Z. Zhang, W. Chen, and Z. Feng, "A novel hybrid-fed patch antenna with pattern diversity," *IEEE Antennas and Wireless Propagation Letters*, vol. 9, pp. 562–565, 2010.

[54] M. Gupta and V. Mathur, "Multiband multiple elliptical microstrip patch antenna with circular polarization," *Wireless Personal Communications*, vol. 102, no. 1, pp. 355–368, 2018.

[55] H. Dashti and M. Neshati, "Design investigation of microstrip patch and half-mode substrate integrated waveguide cavity hybrid antenna arrays," *International Journal of Engineering Transactions B: Basics*, vol. 28, no. 5, pp. 686–692, 2015.

[56] P. Mythili and A. Das, "Theoretical investigations of an annular elliptical ring microstrip antenna using green's function technique," *IEE Proceedings-Microwaves, Antennas and Propagation*, vol. 146, no. 6, pp. 379–384, 1999.

[57] V. Sharma, V. Saxena, K. Sharma, and D. Bhatnagar, "Radiation performance of an elliptical patch antenna with three orthogonal sector slots," *Romanian Journal of Information Science and Technology*, vol. 14, no. 2, pp. 123–130, 2011.

[58] K. Carver and J. Mink, "Microstrip antenna technology," *IEEE Transactions on Antennas and Propagation*, vol. 29, pp. 2–24, January 1981.

[59] W. Richards, Y. Lo, and D. Harrison, "An improved theory for microstrip antennas and applications," *IEEE Transactions on antennas and propagation*, vol. 29, no. 1, pp. 38–46, 1981.

ABSTRACT

DESIGN AND PRACTICAL IMPLEMENTATION OF COMPACT MICROSTRIP ANTENNAS FOR HARMONIC TRANSPONDERS

by

NASSER S ALKHALDI

May 2019

Advisor: Dr. Pai-Yen Chen

Major: Electrical Engineering

Degree: Doctor of Philosophy

Harmonic radar is a nonlinear detection technology that transmits and receives radio-frequency (RF) signals at orthogonal frequencies, so as to suppress the undesired clutters, echoes and electromagnetic interreferences due to multipath scattering. Its implementation generally comprises a nonlinear tag (i.e, a harmonic transponder), which picks the interrogation signal at specific fundamental frequency (f_0) and converts it into a high/sub-harmonic signal (nf_0). Such a technology has been successfully applied to tracking small insects and detection of electrically-small objects in the rich-scattering environment. Similarly, a harmonic sensor is used to interrogate electrically-small and passive sensors, of which the magnitude and peak frequency of output harmonics (e.g., second harmonic) are functions of the parameter to be sensed. A harmonic tag or sensor comprises one or multiple antennas, a frequency modulator, a sensor, a microchip and matching networks. Here, we propose and experimentally validate compact, low-cost, low-profile, and conformal hybrid-fed microstrip antennas for the harmonics-based radar and sensor systems. The proposed microstrip antennas are based on a simple single-layered and hybrid-feed structure. By optimizing the feed position and the geometry of microstrip patch, the fundamental mode and particular higher-order modes can be excited at the fundamental frequency and the second harmonic. We have derived the analytical expressions for calculating the

antennas' resonant frequencies, which have been verified with numerical simulations and measurements. my results show that the proposed hybrid-feed, single-layered microstrip antennas, although having a compact size and a low profile, can achieve descent realized gain (1.2 – 3.5 dB), good impedance matching (return loss < -15 dB), high isolation (<-20 dB), and favorable co/cross-polarization properties. The proposed microstrip antennas may benefit various size-restricted harmonic transponders used for harmonic radars, harmonic sensors, medical implants, passive radio-frequency identification (RFID), and internet-of-things (IoT) applications.

AUTOBIOGRAPHY

Education:

- Current PhD student at Wayne State University, Electrical Engineering Department, since August 26th 2014.
- Master of Science in Network Engineering and Management from DePaul University, Chicago, United States, Fall 2012.
- Bachelor of science in Electrical Engineering from Purdue University, Hammond, United States, Fall 2010.

Work Experience:

- Lecturer at Jubail Industrial College, Electrical and Electronics Engineering Department, Jubail Industrial City, from 03-2013 to present.

Publications:

- Zhu, Liang, Nasser Alkhaldi, Haysam M. Kadry, Shaolin Liao, and Pai Yen Chen. "A Compact Hybrid-Fed Microstrip Antenna for Harmonics-Based Radar and Sensor Systems."*IEEE Antennas and Wireless Propagation Letters* (2018).
- L. Zhu, N. Alkhaldi, and P. Y. Chen, "A Compact Harmonic Sensor Based on a Dual-Resonant Microstrip Antenna Loaded with a Microfluidic Channel," 2019 USNC-URSI National Radio Science Meeting, Boulder, Colorado, January 2019.
- L. Zhu, N. Alkhaldi, M. C. C. Cheng, and P. Y. Chen, "Microfluidic-Integrated, Dual-Resonant Elliptical Microstrip Patch Antennas for Making Compact Harmonic-Transponder Sensors," under preparation.